



MSU Graduate Theses


Spring 2022

Investigation Into Karst of Southwest Missouri Using Electrical Resistivity

Donald Zachary Wormington
Missouri State University, zac0407@live.missouristate.edu

As with any intellectual project, the content and views expressed in this thesis may be considered objectionable by some readers. However, this student-scholar's work has been judged to have academic value by the student's thesis committee members trained in the discipline. The content and views expressed in this thesis are those of the student-scholar and are not endorsed by Missouri State University, its Graduate College, or its employees.

Follow this and additional works at: <https://bearworks.missouristate.edu/theses>

 Part of the [Geology Commons](#), [Geophysics and Seismology Commons](#), and the [Speleology Commons](#)

Recommended Citation

Wormington, Donald Zachary, "Investigation Into Karst of Southwest Missouri Using Electrical Resistivity" (2022). *MSU Graduate Theses*. 3763.
<https://bearworks.missouristate.edu/theses/3763>

This article or document was made available through BearWorks, the institutional repository of Missouri State University. The work contained in it may be protected by copyright and require permission of the copyright holder for reuse or redistribution.

For more information, please contact bearworks@missouristate.edu.

**INVESTIGATION INTO KARST OF SOUTHWEST MISSOURI USING ELECTRICAL
RESISTIVITY**

A Master's Thesis

Presented to

The Graduate College of

Missouri State University

In Partial Fulfillment

Of the Requirements for the Degree

Master of Science, Geography and Geology

By

Donald Zachary Wormington

May 2022

The author assumes responsibility for obtaining and maintaining the necessary rights and releases to legally publish this work, including the informed consent of any subjects identifiable in the photographic and/or illustrative work.

INVESTIGATION INTO KARST OF SOUTHWEST MISSOURI USING ELECTRICAL RESISTIVITY

Geography, Geology, and Planning

Missouri State University, May 2022

Master of Geography & Geology

Donald Zachary Wormington

ABSTRACT

Nixa, Missouri is located on the southwestern edge of the Ozark Dome which has a karst geomorphological environment. Near surface geophysical methods can be used in determining the location and nature of karst features such as caves and sinkholes. Electrical resistivity methods have been shown to be among the most useful methods in deciphering sinkholes and caves. To investigate a known cave and related sinkholes and faults within Mississippian carbonates south of Nixa, Missouri, a series of two-dimensional electrical resistivity profiles were collected using the dipole-dipole and Schlumberger arrays. Terrain data was collected to include in modeling. The data were modeled using a robust two-dimensional inversion method where the inversion parameters were varied to determine the statistically most reasonable model. Using these methods new unexplored cave passages have been detected around the existing cave. The data collect has been used to estimate the location and dimensions of these new cave passages. These new cave passages were found to the northwest and northeast of the known cave passages.

KEYWORDS: karst, resistivity, sinkhole, geophysics, cave

**INVESTIGATION INTO KARST OF SOUTHWEST MISSOURI USING
ELECTRICAL RESISTIVITY**

By

Donald Zachary Wormington

A Master's Thesis
Submitted to the Graduate College
Of Missouri State University
In Partial Fulfillments of the Requirements
For the Degree of Master of Science, Geography & Geology

May 2022

Approved:

Kevin L. Mickus, D.G.S., Thesis Committee Chair

Douglas R. Gouzie, Ph.D., Committee Member

Melida Gutierrez, Ph.D., Committee Member

Julie Masterson, Ph.D., Dean of the Graduate College

In the interest of academic freedom and the principle of free speech, approval of this thesis indicates the format is acceptable and meets the academic criteria for the discipline as determined by the faculty that constitute the thesis committee. The content and views expressed in this thesis are those of the student-scholar and are not endorsed by Missouri State University, its Graduate College, or its employees.

ACKNOWLEDGEMENTS

I would like to thank my thesis committee for helping me through my research; Dr. Kevin Mickus, for guidance on geophysical methods and processing; Dr. Douglas Gouzie, for his guidance on karst hydrology, finding this research topic; and Dr. Melida Gutierrez for her guidance in thesis writing and formatting. I would like to thank Moamen Almaz for helping with fieldwork. I would like to thank and acknowledge Ophelia Pettus for her help in the field and with edits as well as her support financially and mentally. I also would like to thank the owner of the studies cave for allowing access to the cave and its surrounding properties.

TABLE OF CONTENTS

Introduction	Page 1
Study Area	Page 7
Cave Geology	Page 8
Topography	Page 8
Geology	Page 18
Focus Areas	Page 24
Methods	Page 28
Geospatial Information Systems	Page 28
Electrical Resistivity	Page 30
Results	Page 41
Area 1 – Known Cave Under Large and Small Sinkholes	Page 41
Area 2 – Long Crawl Cave	Page 46
Area 3 – East of Main Cave and Large Sinkholes	Page 50
Area 4 – Small Sinkhole Northwest of Main Cave Chamber	Page 59
Discussion	Page 66
Conclusions	Page 69
References	Page 70

LIST OF FIGURES

Figure 1. Evolution of Typical Sinkhole	Page 2
Figure 2. Saturation Concentration	Page 3
Figure 3. Summary of Cave Patterns	Page 5
Figure 4. Geological Map of Missouri	Page 7
Figure 5. Cave Map	Page 9
Figure 6. Large Chamber in Northern Section	Page 10
Figure 7. Large Chamber in Eastern Section	Page 11
Figure 8. Nearly Obstructed Passage	Page 12
Figure 9. Large Breakdown	Page 13
Figure 10. Hillshade of Greater Study Area	Page 14
Figure 11. Cave Entrance	Page 15
Figure 12. Large Sinkhole	Page 16
Figure 13. Small Sinkhole	Page 17
Figure 14. Stratigraphic Column of Southwest Missouri	Page 19
Figure 15. Pierson Formation Sample	Page 20
Figure 16. Northview Formation Sample	Page 21
Figure 17. Compton Formation Sample	Page 22
Figure 18. Bachelor Formation Sample	Page 23
Figure 19. Major Fault Trends of Southwest Missouri	Page 24
Figure 20. Focus Areas Highlighted	Page 25
Figure 21. Reach RS2 GNSS Receiver	Page 28

Figure 22. Topcon GPS	Page 29
Figure 23. Illustration of Ohm's Law	Page 30
Figure 24. Illustration of Resistivity	Page 31
Figure 25. Electrical Current Flow Lines	Page 32
Figure 26. High and Low Resistivity Bodies	Page 33
Figure 27. ARES System	Page 36
Figure 28. Supersting R8	Page 37
Figure 29. Data Point Distribution	Page 39
Figure 30. Area 1	Page 41
Figure 31. Line 1	Page 43
Figure 32. Line 2	Page 44
Figure 33. Line 3	Page 45
Figure 34. Line 4	Page 47
Figure 35. Area 2	Page 48
Figure 36. Line 5	Page 49
Figure 37. Line 6	Page 51
Figure 38. Area 3	Page 52
Figure 39. Line 7	Page 53
Figure 40. Line 8	Page 55
Figure 41. Line 9	Page 56
Figure 42. Line 10	Page 57
Figure 43. Line 11	Page 58
Figure 44. Area 4	Page 60

Figure 45. Line 12	Page 61
Figure 46. Line 13	Page 62
Figure 47. Line 14	Page 64
Figure 48. Line 15	Page 65
Figure 49. Predicted Subsurface Void Locations	Page 67

INTRODUCTION

Karst is a type of topography that is formed over limestone, dolomite, or gypsum by dissolution, and that is characterized by sinkholes, caves, and underground drainage (Bates and Jackson, 1984). Karst lends itself readily to the formation of unique surface and subsurface features. Fractures and/or bedding planes in the subsurface of karst can become widened by dissolution, resulting in the formation of voids in the subsurface. These voids form when surface and groundwater infiltrate into soluble bedrock and flow through fractures or bedding planes present in the subsurface dissolving the bedrock and then transporting the dissolved material away. Bedrock permeability, which is the ability of water to be transported through the subsurface, is drastically increased by the presence of faults and the fractures. This is important for the formation of karst features because there must be a constant recharge of water to the subsurface in order for karst features to continue to grow from dissolution.

As water dissolves the bedrock along fractures and bedding planes, the small voids that allow for the flow of slightly acidic water slowly increase in dimension over time (Palmer, 1991). When one of these subsurface voids grows large enough and breaches the surface a cave is formed. As the permeability of the subsurface increases and the voids in the subsurface grow, the flow through the void can be described as an underground river. This helps increase the size of voids and the rate of dissolution as water easily enters and then subsequently exits the subsurface. Places where water is able to enter the voids in the subsurface often begin to form cone-shaped depressions that are visible on the surface. These cones are places where water could not flow over the surface terrain, yet no standing water is present. When this occurs, a sinkhole is formed. (Figure 1) (Qiu et al., 2018) These sinkholes often form slowly as the

overlying debris and soil channel the water to be drained into the void, slowly expanding its parameters (Berglund et al., 2014). Sinkholes can also appear suddenly when collapse occurs in the subsurface caused by the roof of a void in the subsurface falling in on itself. Streams can enter the subsurface through these and other entry points, and then exit the subsurface where they will continue as surface flow. These places where streams re-emerge at the surface are known as springs. (Palmer, 1991).

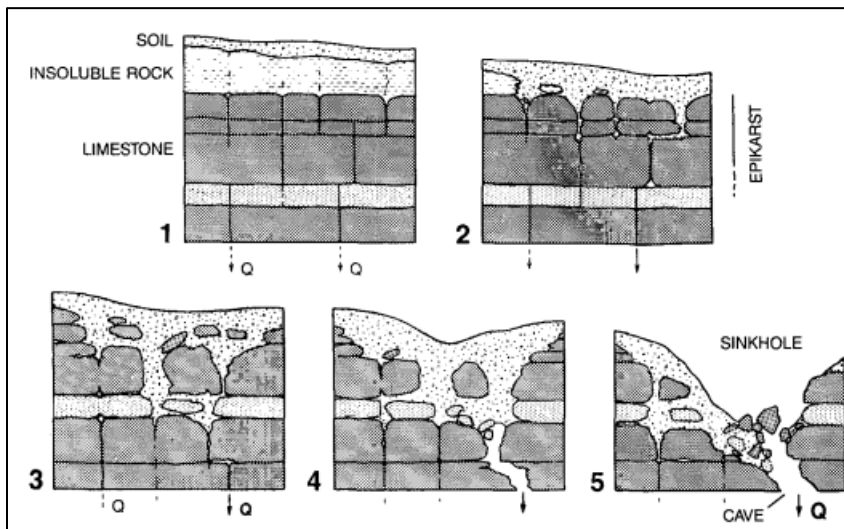


Figure 1. Evolution of a typical sinkhole in a karst environment. (Palmer, 1991)

The karst features that form in southwest Missouri forms for three specific reasons. First, the subsurface is soluble. This is because the geology predominant in this area consists mostly of Mississippian aged limestones and dolomites. This carbonate lithology dissolves readily when exposed to rain and ground water that is slightly acidic due to mixing with CO₂. Secondly, acidic water frequently comes into contact with the bedrock. Rainwater becomes acidic due to absorption of CO₂ as it travels through the air during rainfall as well as when it percolates through the soil as it travels to the bedrock. The climate in southwest Missouri is that of a

temperate continental environment. Its precipitation seasonality is less pronounced than the northern part of the state due to subtropical airmasses throughout the year (Decker, 2022). This causes the subsurface to receive rainwater recharge year-round. Lastly, the acidic rainwater is able to enter and exit the soluble subsurface through the fractures and bedding planes in the subsurface. It is important that the water is able to enter and subsequently exit the bedrock. If the water is only able to come into contact with the soluble rocks from the surface then it will only be able to erode from the top down and karst features will have difficulty forming. Water is also only able to dissolve minor amounts of carbonate rock before it becomes saturated (Figure 2), so drainage is of vital importance to the continued dissolution of the subsurface karst features. (White, 2002).

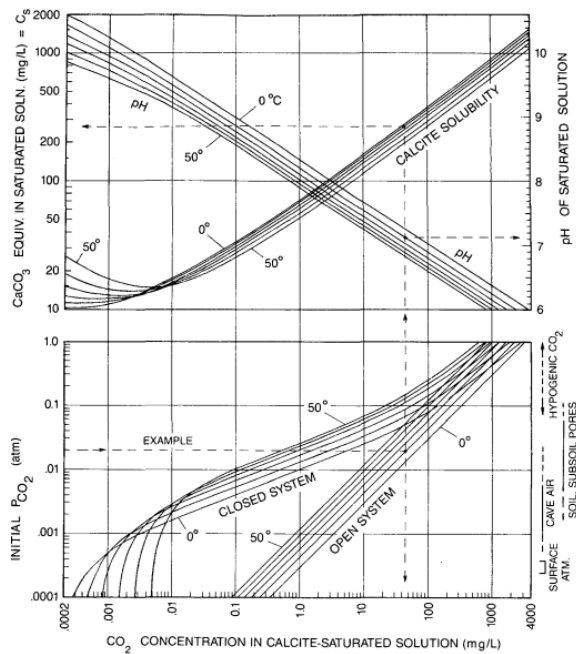


Figure 2. Saturation concentration of dissolved calcite, versus initial, equilibrium CO₂. And equilibrium pH. Modified from Palmer. (1991)

How ground water flows through a karst environment is one of the more difficult aspects to investigate in studying a karst environment. This is due to the fact that the majority of the factors that influence this flow are not observable from the surface. The layers in the bedrock can cause the water to flow horizontally through the subsurface when it would normally flow vertically. Likewise vertical fractures can cause water to flow vertically when it would normally trend horizontally. This is because fractures and bedding planes become the areas of least resistance to flow in the bedrock. While one of these areas of least resistance may be the dominate factor in determining the formation of voids in the subsurface, often it is a combination of these factors working together at different angles and orientations that cause the subsurface voids to acquire their specific shapes.

Sinkholes, especially collapse sinkholes can be extremely hazardous to human infrastructure. Slowly forming sinkholes can interfere with the stability of a building and roads. While large sinkholes formed from collapse are capable of destroying entire buildings in an instant (Gouzie and Pendergrass, 2009). Construction over these karst areas normally involve investigation into the existing karst features that could pose a potential future threat. Since voids in the subsurface that collapse can be the cause of these potentially dangerous sinkholes that form, an understanding of how these voids form and evolve is essential to the safe existence of society in karst areas.

Cave formation in karst follows the trends of the surrounding subsurface features, but an accurate prediction model of a specific cave's recharge and formation pattern does not exist (Figure 3). This is due to the uniqueness of each karst system and the unpredictability of the fractures and bedding planes in a specific area that facilitate the unpredictable formation of a cave (Palmer, 1991). So, while trends in known caves and karst features can aid in the discovery

of new subsurface voids, actual detection methods need to be employed to determine the existence of said voids. Even the exact location of previously known voids can change or become lost due to the sudden collapse of cave roofs, requiring redetection.






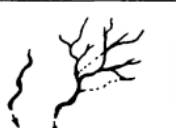

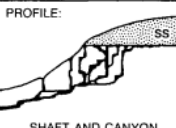
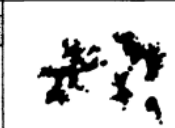

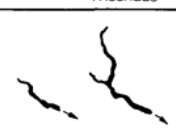

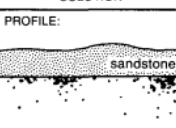
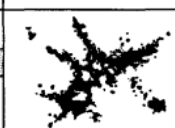
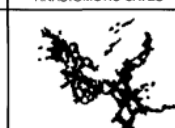
		TYPE OF RECHARGE					
		VIA KARST DEPRESSIONS		DIFFUSE		HYPOGENIC	
		SINKHOLES (LIMITED DISCHARGE FLUCTUATION)	SINKING STREAMS (GREAT DISCHARGE FLUCTUATION)	THROUGH SANDSTONE	INTO POROUS SOLUBLE ROCK	DISSOLUTION BY ACIDS OF DEEP-SEATED SOURCE OR BY COOLING OF THERMAL WATER	
DOMINANT TYPE OF POROSITY		BRANCHWORKS (USUALLY SEVERAL LEVELS) & SINGLE PASSAGES		SINGLE PASSAGES AND CRUDE BRANCHWORKS, USUALLY WITH THE FOLLOWING FEATURES SUPERIMPOSED:	MOST CAVES ENLARGED FURTHER BY RECHARGE FROM OTHER SOURCES	MOST CAVES FORMED BY MIXING AT DEPTH	
DOMINANT TYPE OF POROSITY	FRACTURES	 ANGULAR PASSAGES	 FISSURES, IRREGULAR NETWORKS	 FISSURES, NETWORKS	 ISOLATED FISSURES AND RUDIMENTARY NETWORKS	 NETWORKS, SINGLE PASSAGES, FISSURES	
	BEDDING PARTINGS	 CURVILINEAR PASSAGES	 ANASTOMOSES, ANASTOMOTIC MAZES	PROFILE:  SHAFT AND CANYON COMPLEXES, INTERSTRATAL SOLUTION	 SPONGEWORK	 RAMIFORM CAVES, RARE SINGLE-PASSAGE AND ANASTOMOTIC CAVES	
	INTERGRANULAR	 RUDIMENTARY BRANCHWORKS	 SPONGEWORK	PROFILE:  RUDIMENTARY SPONGEWORK	 SPONGEWORK	 RAMIFORM & SPONGEWORK CAVES	

Figure 3. Summary of cave patterns and the relationship they have to recharge and porosity. These are general representations of cave types. Real world caves are a combination of one or more of the above patterns. Modified from Palmer (1991).

In karst areas, one of the largest challenges to research and planning is the uniqueness of each area. No two karst regions are exactly alike and the factors that determine the growth of karst features can vary drastically within the same region (Berglund, 2012). One of the goals of this thesis is to help compare the logistics and usefulness of geophysical methods to investigate karst. As well as testing the ability of these techniques to detect large and small subsurface voids within the same karst area. In this study, the electrical resistivity method will be used.

The objectives of this research project are to:

- Investigate karst features using electrical resistivity methods
- Explore usefulness of electrical resistivity to determine karst features
- Determine if voids of different sizes in the subsurface can be detected using geophysical methods
- Determine if detected voids are connected to and contribute to the main cave system
- Create a new model of the cave system that incorporates these new voids and summarize local karst characteristics within the study area

STUDY AREA

The study area is in Stone County, Missouri, on the southern edge of the Ozark dome (Figure 4). The cave exists in the Pierson Formation, a Mississippian aged limestone of southwest Missouri. The cave is a former show cave with a storied history that the current owner would like to keep private. As such no further description of physical location of the study area will be given other than its general location in southwest Missouri.

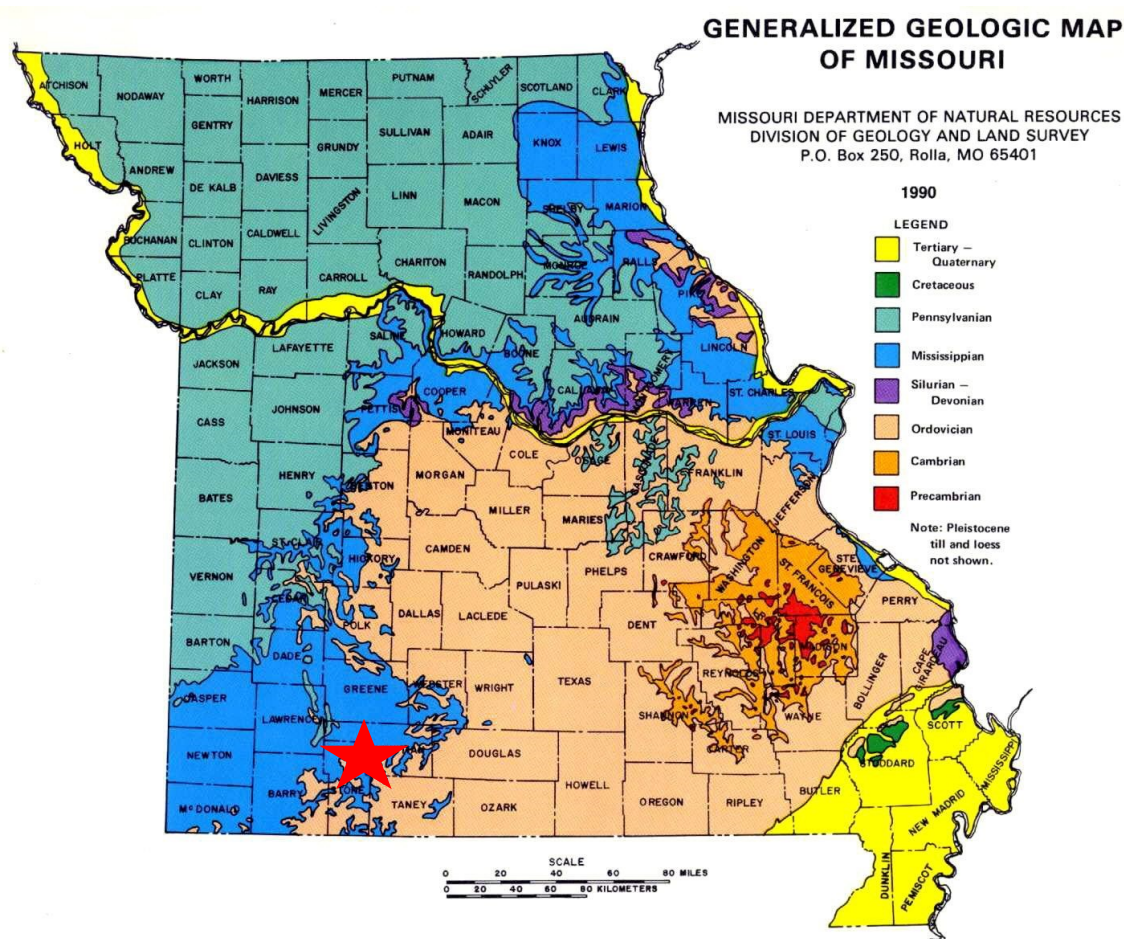


Figure 4. Geological map of Missouri. Red star indicates general location of the study area. (Evans et al., 2011)

Cave Geology

The cave (Figure 5) being studied is currently closed to the public and gated off. Small parts of the cave have been paved and otherwise modified for human exploration. The cave itself is a solutional cave that follows fracture trends in the subsurface and takes up roughly 150m by 150m in the subsurface. The general shape of the cave is characterized by several large open chambers ranging from roughly 10m³ to 30m³ connected by smaller conduits that have a few meters of clearance or less and can be several meters in length. Many of the main large chambers (Figures 6 and 7) have floors covered in debris ranging from small pebble sizes up to large boulders several meters across (Beard, 2019). The entrance to many of the smaller passages have been obscured by large boulders that were once a part of the cave's ceiling (Figures 8 and 9). The cave was last open to the public in the mid-1900s. The current owner is interested in determining if any other voids in the subsurface could be excavated to in order to increase the dimensions of the current known cave.

Topography

The study area (Figure 10) is a roughly a 0.6 by 0.6 km square area in the northern portion of Stone County. Elevation trends from 410m in the northwest to 350m in the southeast portions of the area. The highest elevation is 412m above sea level near the center of the study area and the lowest elevation is 350m above sea level in the stream valley that the cave spring empties into in the southwest corner of the study area. A large cliff (Figure 11) that is roughly 30m in relief extends from east to west in the southern portion of the study area. This cliff contains the main entrance into the cave. Above the cliff, near the center of the study area, there are two large sinkholes that are easily seen on the surface. The larger of the two (Figure 12) is situated in line with the cave entrance and is 90m north of the cliff face. The smaller of the two sinkholes

(Figure 13) is offset to the northwest from the larger sinkhole by 15m and is 30m to the north from it. The cones the sinkholes form over roughly a 15m by 15m and 10m by 10m area respectively.

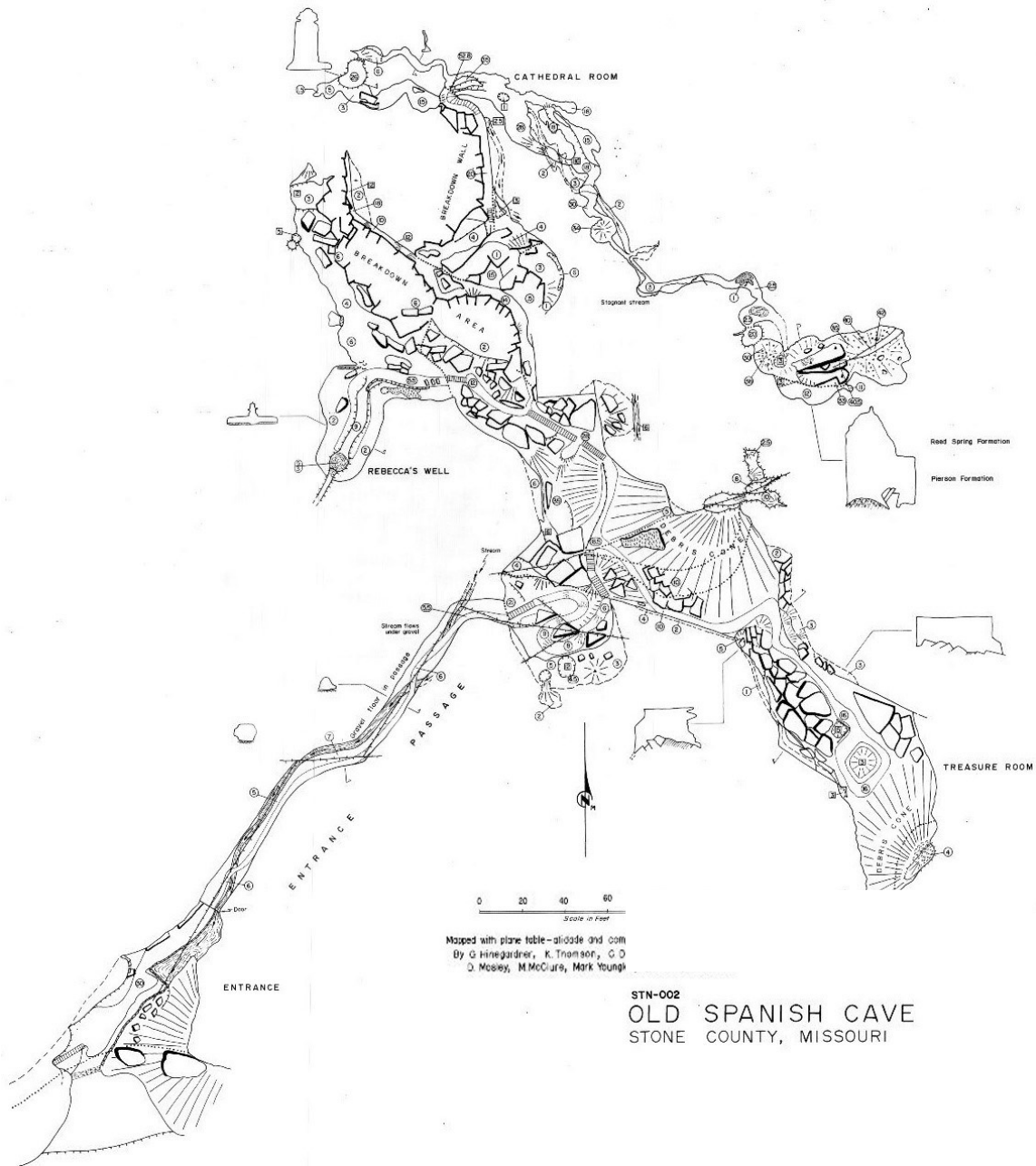


Figure 5. Map of the cave being studied with name and identifying notations redacted. Obtained from cave owner via written correspondence.



Figure 6. Large chamber in the northern section of the cave.



Figure 7. Large chamber in the eastern portion of the cave.



Figure 8. Breakdown within cave that nearly blocks passage entrance.



Figure 9. Large debris blocks in the large chamber of the cave. The main block shown is approximately 6 meters tall.

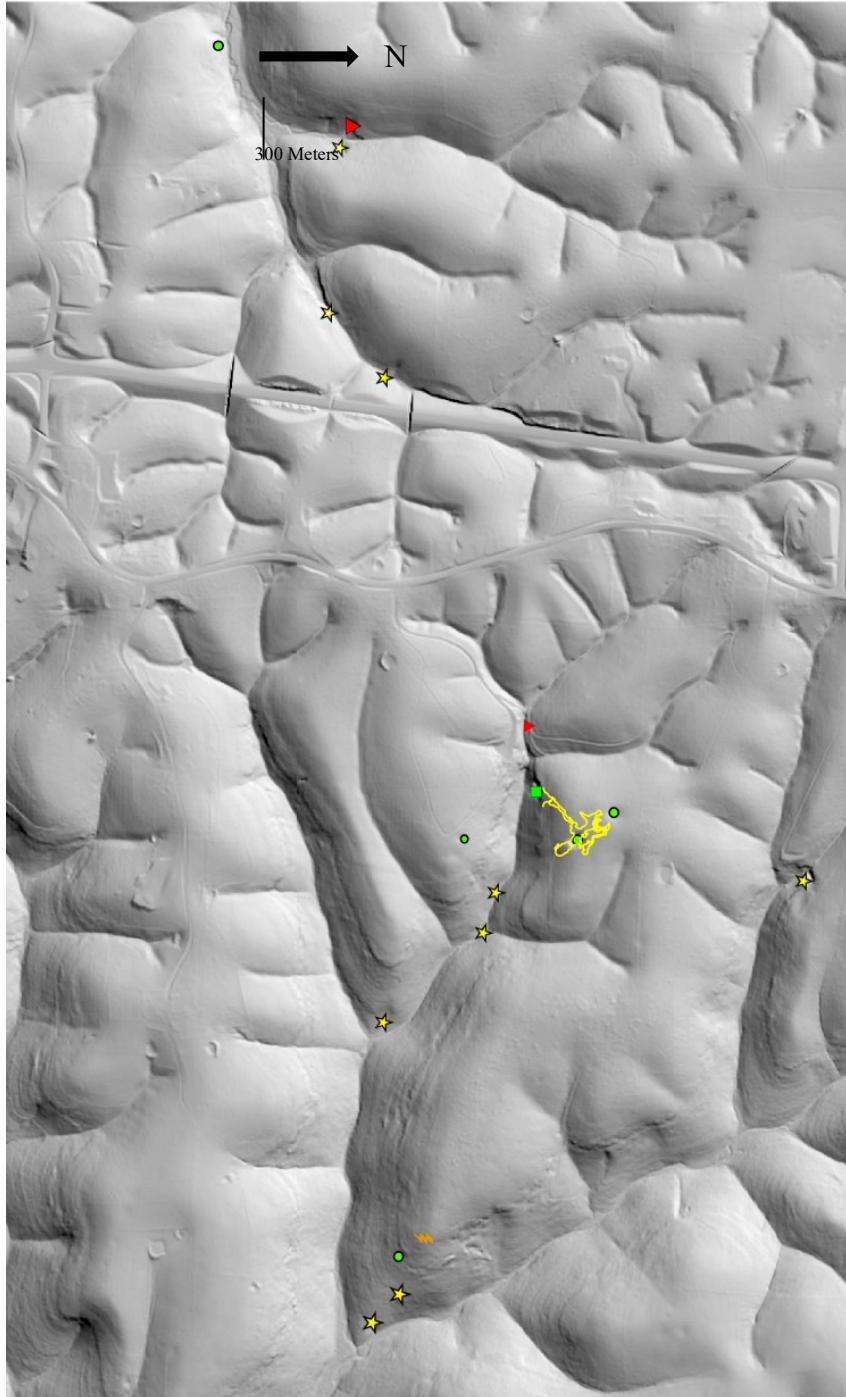


Figure 10. Hillshade of the greater study area with yellow outline of cave map from Figure 5. Red triangles represent locations of small cave openings on the property. The green dots are the locations of sinkhole cones visible on the surface. The green square is the main cave entrance. The yellow stars are cave openings of interest. The brown lightning bolt is a powerline tower.



Figure 11. Main entrance of the cave that is in the large cliff face.



Figure 12. Large sinkhole above cave.



Figure 13. Small sinkhole above cave.

Geology

The geology and stratigraphy (Figure 14) of the Stone County cave area has the Pierson formation (Figure 15) as the main rock type. The Pierson Limestone is a crinoidal packstone to wackestone. Chert nodules left from the eroded Reed Spring Formation cover the Pierson formation in the study area. There are also small patches of soil and exposed epi-karst. The Pierson is nearly horizontally oriented with a slight tilt of less than 1 degree to the southwest and is up to 21m thick in the study area. Beneath the Pierson Formation is the Northview Formation (Figure 16). The Northview Formation is a confining layer in southwest Missouri. The Northview Formation is a gray-green siltstone and shale formation. The Northview Formation ranges from a few feet thick to non-existent in the study area. The known cave passages sit atop the Northview Formation and cut down through it in places. The formation below the Northview Formation and last karst bearing formation in the study area is the Compton formation. The Compton Formation (Figure 17) is another crinoid packstone to wackestone. The Compton Formation is up to 20 meters thick in the study area, where the bottom can be seen. The Compton Formation is underlain by the last relevant formation in the study area, the Bachelor Formation (Figure 18). The Bachelor Formation is a sandstone and shale. The Bachelor Formation acts as a confining unit hampering the formation of karst below its location. The Pierson and Compton Formations are both highly susceptible to karst development and contain many caves, and sinkholes. The Pierson Formation is not the only rock unit to outcrop in the study area, though it is the dominant. The large cliff face containing the main cave entrance provides an outcrop showing all the above units displayed openly and in order (Thompson, 1986).

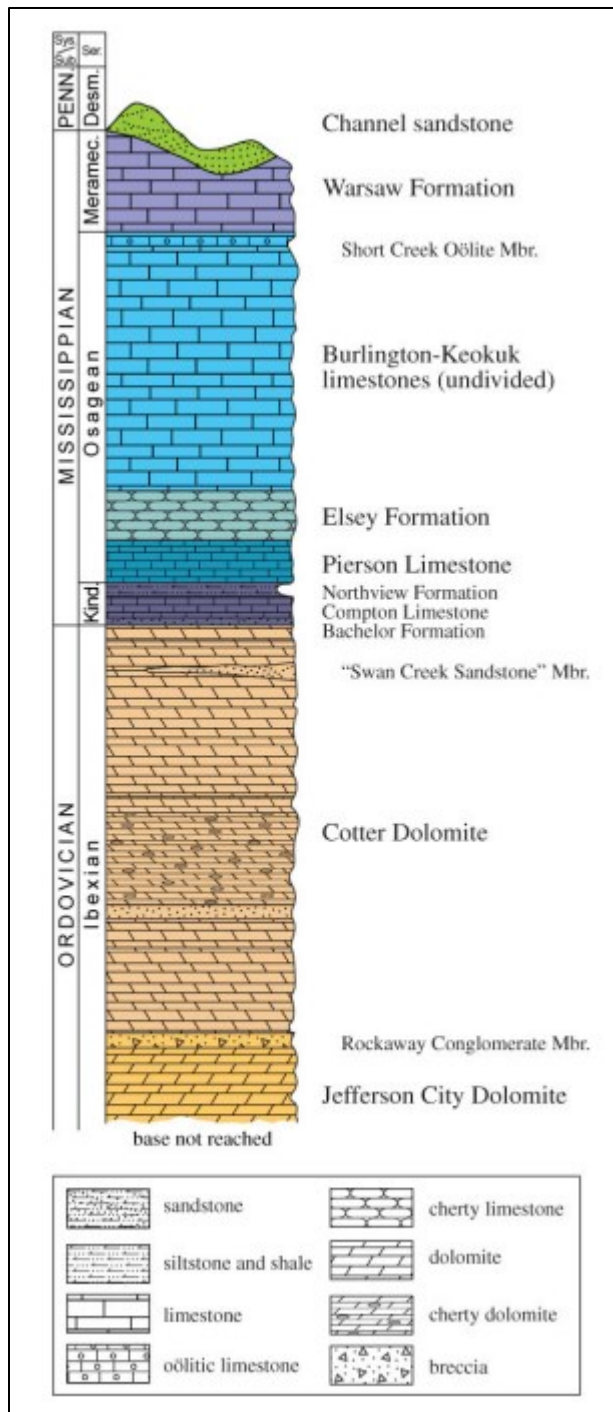


Figure 14. Stratigraphic column of southwest Missouri. (Evans et al., 2011).



Figure 15. A hand sample of the Pierson Formation.



Figure 16. A hand sample of the Northview formation.



Figure 17. Hand sample of the Compton formation.



Figure 18. Hand sample of the Bachelor Formation.

The rock units in southwest Missouri are all nearly horizontal with a general regional northwest to southwest dip of less than 1 degree. The small amount of structural deformation within the rock layers can be seen as northwest to southeast trending faults and fractures (Figure 19). The age of this faulting is uncertain, but the consensus associates the faults with the Ouachita Orogeny from the Pennsylvanian time period (Evans et al., 2011). The passages in the known cave from the study area generally follow this same northwest to southeast trend. With

parallel connecting passages forming mostly along the bedding plane between the Pierson and Compton where the Northview is not present.

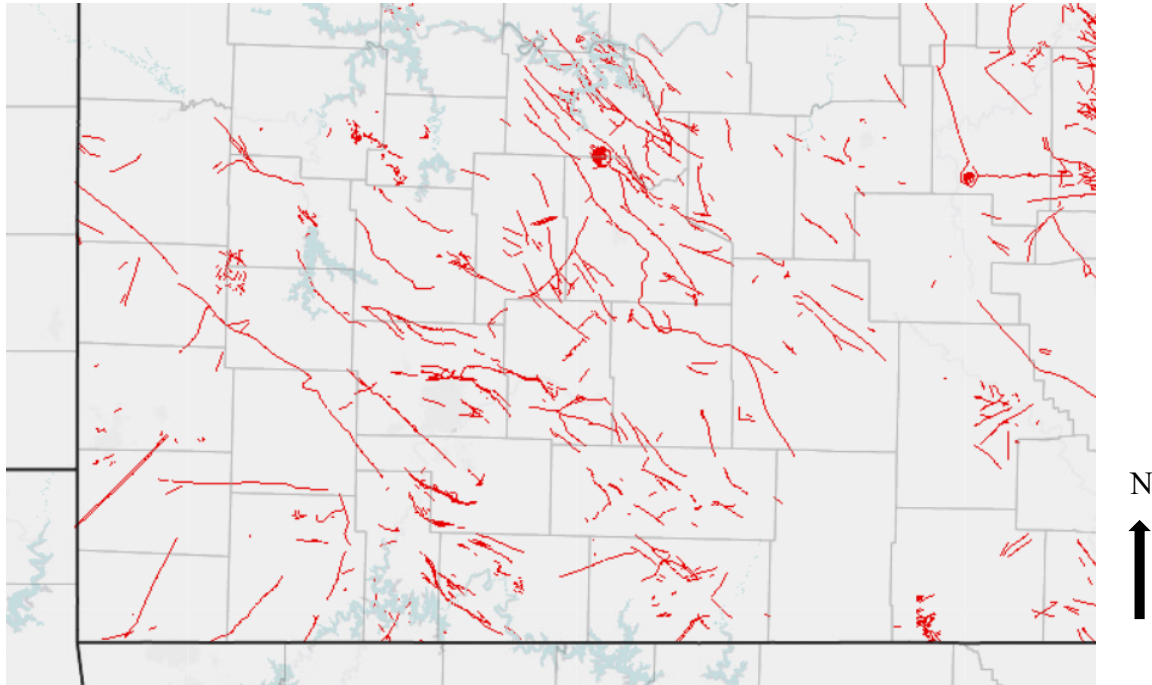


Figure 19. Major fault trends of southwest Missouri.

Focus Areas

Within the larger study area four main areas of focus were selected (Figure 20) based on their likelihood to contain possible unmapped voids that could potentially be associated with the current known cave. These sites were selected based on accessibility, information obtained using GIS data, information obtained during a field expedition to the site, and information gathered from the owner of the property containing the cave.



Figure 20. The greater study area with the four smaller focus areas highlighted. Area 1 is highlighted in yellow. Area 2 is highlighted in red. Area 3 is highlighted in orange. Area 4 is highlighted in blue. The yellow outline is the cave map from Figure 5. Red triangles represent locations of small cave openings on the property. The green dots are the locations of sinkhole cones visible on the surface. The green square is the main cave entrance. The yellow stars are cave openings of interest. The brown lightning bolt is a powerline tower.

Area 1 – Known Cave under large and small Sinkholes. The first and most likely of the areas to return good usable data is the area directly above the known cave. This site was selected to give a baseline reading to use as a metric for all of the other areas. Both large sinkholes above the cave and the presence of the known cave may return results usable as a metric for the investigation in the surrounding areas. All other data collected will be compared with the data from this central site to help verify the obtained results.

Area 2 – Long Crawl Cave Connection. The first and least likely of the four to connect to the known cave is also the furthest from the cave. The study area is located near a highway that splits the property belonging to the cave's owner. The larger property as a whole contains more than one known cave. One of these caves is a long straight southwest to northeast trending cave that follows the bedding plane between the top of the Northview Formation and the bottom of the Pierson Formation. The trend of the long crawls nearly 200m passage lines up with the main chamber of the study cave. There is a story obtained by the owner of a neighbor crawling through long crawl cave and emerging in the study cave over 50 years ago. The long crawl's location being 1km away does however make this connection unlikely.

Area 3 – Area East of Main Cave Chamber and Large Sinkhole. The second of the four locations chosen for this study is the area west of the large sinkhole associated with a debris cone in the main chamber of the cave. The area to the east can be split into two smaller subsections. The northern half being associated with the majority of the knob containing the known cave. The knob created by three drainage valleys is larger than the study area, but the highpoint and center of the knob is located just to the northeast of the large sinkhole on the surface. This leaves a large area in the subsurface of karst susceptible rock that may contain voids that could possibly be connected with the main cave. The area to the southeast of the large

sinkhole on this knob is punctuated by a spring that comes out of the cliffside in the drainage valley. This spring runs slowly year-round and may be associated with an underground stream within the known cave that disappears flowing to the southeast within the cave. A void connecting this spring and the known cave is possible.

Area 4 – Small Sinkhole Northwest of Main Cave Chamber. The third location was selected because the entrance to the northernmost chamber in the cave is nearly blocked by a debris cone possibly associated with the smaller of the two large sinkholes located above the cave. Though the passage is accessible north of the debris cone, access to a possible western chamber may be blocked. The debris cone is not yet confirmed to be associated with the smaller sinkhole. Confirmation of this connection and identification of possible voids beyond the current confines of the cave seem likely at this location.

METHODS

Geospatial Information Systems (GIS)

GIS Data Collection. The Missouri Spatial Data Information Service (MSDIS) was used to obtain the majority of the data. The data sets include hillshades and elevation models, topographic information of the study area, stream locations, sinkhole locations, spring locations, fault and fracture locations, roads and highway information, and geopolitical boundaries. Satellite imagery of the study area was obtained from Google Earth. Geospatial field data collected from a Reach RS2 GNSS Receiver (Figure 21) and a Topcon Gps (Figure 22). To gather the absolute elevation and terrain data.



Figure 21. Reach RS2 GNSS Receiver



Figure 22. Topcon GPS

GIS Data Implementation. ArcGIS 10 and Google Earth were used for geospatial analysis and map production. These applications were used to better correlate the visible surface features with the known and unknown subsurface features identified using various geophysical methods. GIS data allowed the location of geophysical surveys to be planned and executed more efficiently. Contouring of geophysical point data allowed for the production of spatial geophysical maps.

GIS Applications in Karst. GIS data have been used to great success in all areas of geology, including karst geology. GIS data are useful for locating and correlating karst features visible on the surface. Studies into karst have partly been to help better understand the development and prediction of hazards associated with karst such as sinkholes (Gao, 2008).

Ground water studies also show the correlation between disappearing streams and springs with possible underground streams. From this, it could be inferred that areas of mapped sinkholes and springs may be associated with unmapped voids in the subsurface (Florea, 2005).

Electrical Resistivity

ER Theory. The electrical resistivity (ER) method is an active geophysical method used to detect near surface features (Loke, 2020). The method uses Ohm's Law where the current (I) in amps, flowing between two points is equal to the potential difference (V) in volts, divided by the resistance (R) (Figure 23).

$$I = \frac{V}{R}$$

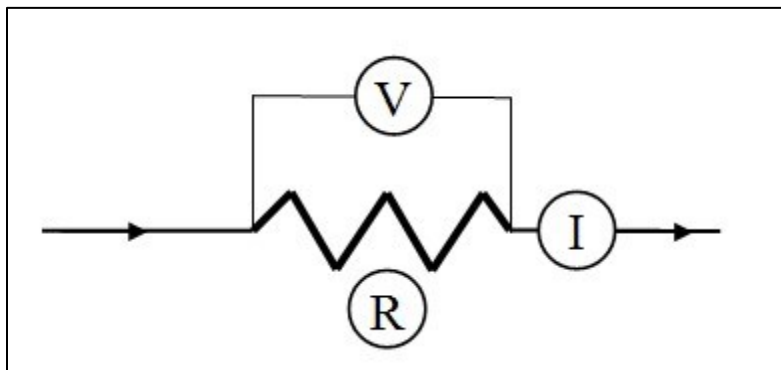


Figure 23. Illustration of Ohm's law where R is the resistivity, I is the current, and V is volts.

Electrical resistance (R) is a function of length (L) of material, resistivity (ρ) in ohms per length, and cross-sectional area (A) of a given material the current is flowing through (Figure 24).

$$R = \frac{\rho L}{A}$$

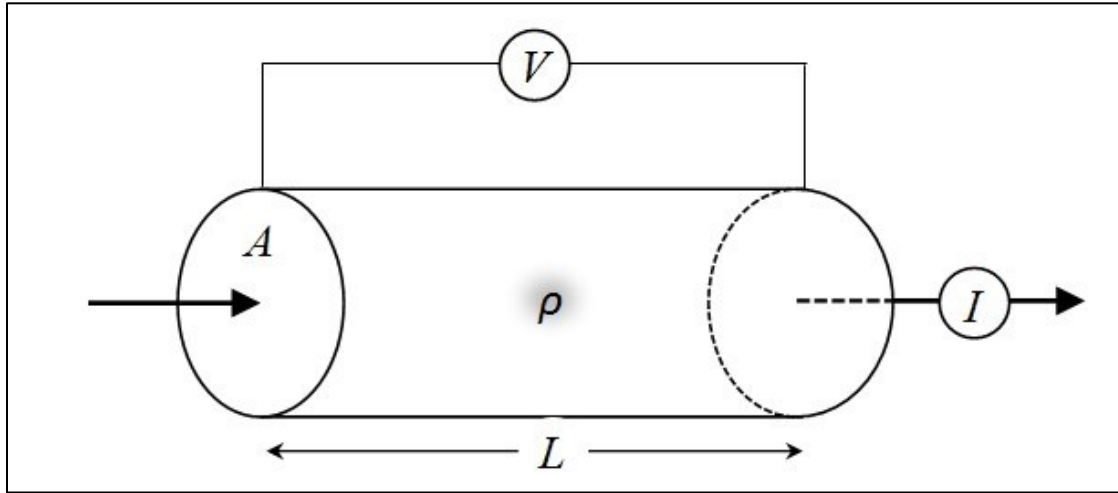


Figure 24. Illustration of resistivity (ρ) of a material, where A is the area, I is the current, V is the voltage potential, and L is the length of a material.

When these equations are combined, the resistivity (ρ) of a material can be calculated. Knowing the current (I), the voltage potential (V), the area (A), and length (L) of a material, a current is flowing through, the resistivity of the material can be found.

$$\rho = \frac{VA}{IL}$$

If an electrical current flows from one electrode to another electrode in a straight line, this equation would fully apply to electrical resistivity survey. When flowing within a homogeneous material, electrical current flows out in all directions as a hemisphere in the Earth. (Figure 25).

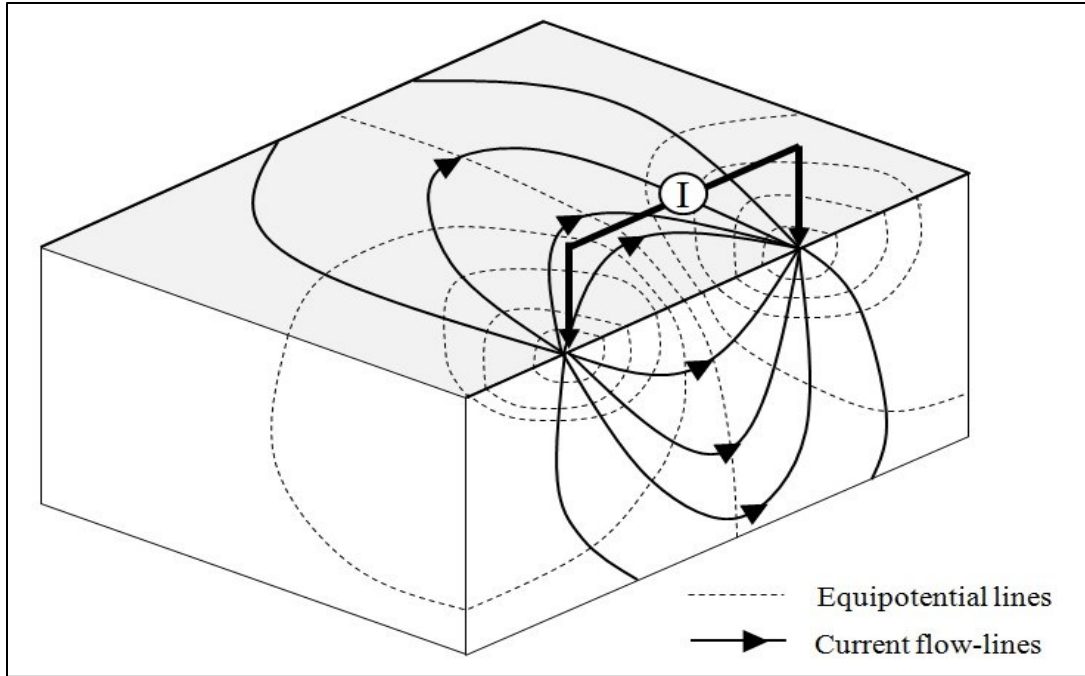


Figure 25. 3D illustration of electrical current flow lines and equipotential fields 3D block.

Whenever an ER survey is undertaken, electrical current always flows from one current electrode to a second. This produces electrical equipotential lines in the subsurface. These lines can be measured on the surface using two or more potential electrodes. If electrical current passes through a highly resistive body, this produces a drop in measured voltage potential at these surface potential electrodes. A low resistivity body results in the opposite effect (Figure 26).

In this equation, the terms A and l are defined by the shape and size of the hemisphere. This is determined by the spacing of the current electrodes placed in the ground. As well as the point in the sphere at which the potential is measured using the potential electrodes. A geometric factor (K) is then substituted in place of length (L) and cross-sectional area (A) to calculate resistivity (ρ) for any given electrode configuration.

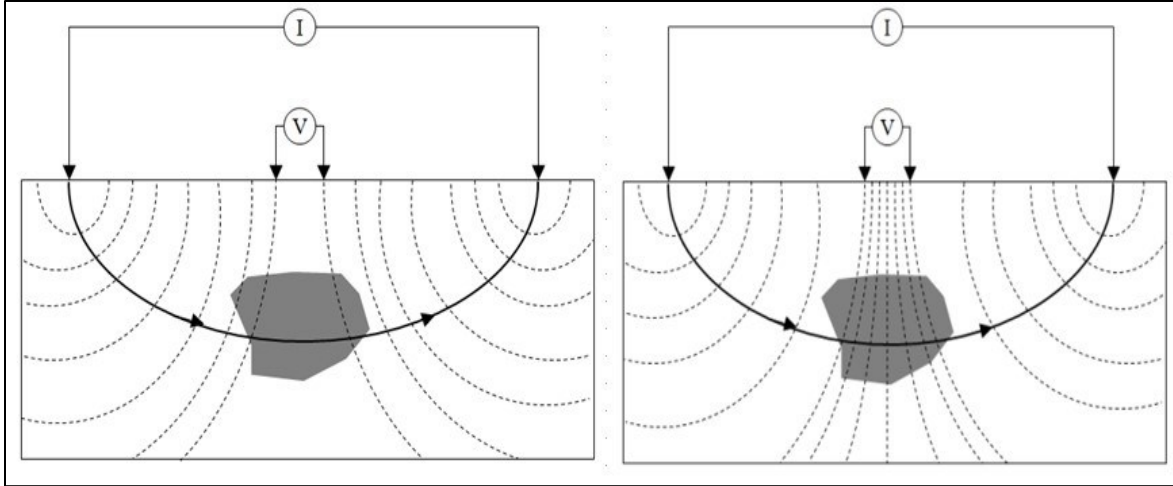


Figure 26. Cross-section illustrations of how a low resistivity (left) or high resistivity (right) subsurface body would result in different measured voltage potential drops at the surface. I-current, V-voltage potential.

$$\rho = RK$$

Geometric factors are defined for a number of arrays which allows for a simple substitution into the above equation. For this study, electrical resistivity surveys are performed using the geometric factor (K) for the Schlumberger array and the dipole-dipole array.

$$\rho_a = \frac{\pi \left(\frac{s^2 - a^2}{4} \right)}{a} \frac{\Delta V}{I}$$

$$\rho_a = \pi n(n+1)(n+2)a \frac{\Delta V}{I}$$

The Schlumberger array utilizes four electrodes placed with a common midpoint. The two outer electrodes are A and B while the two inner electrodes are M and N. Electrodes A and

B are the current electrodes, while electrodes M and N are the potential electrodes. During a survey the two current electrodes are moved outward from the center point while the two potential electrodes remain stationary. This is continued until the observed voltage between M and N becomes too small, at which point the potential electrodes are moved outward to a new spacing.

The dipole-dipole array has a pair of current electrodes labeled A and B. The array potential electrodes pair are labeled M and N. The apparent resistivity or weighted average of the resistivities under the four electrodes is obtained midway between the two pairs. The depth of the apparent resistivity reading is equal to half the distance between the two dipoles.

ER Applications in Karst. ER surveys have been used in a number of situations and have been proven reliable even in underwater investigations (Dahlin and Loke, 2018; Loke, 2020). ER surveys are one of the most reliable and widely used forms of karst geophysical investigation used (Roth et al., 2002; Zhou et al., 2000). It has been verified that multi-electrode resistivity surveys are reliable to determine depth to bedrock in thinly mantled karst (Roth et al., 2002; Zhou et al., 2000). What was once a time and labor-intensive surveying method has been simplified due to recent advances in both data acquisition and processing. One dimensional surveys requiring manual calculation and master curve matching have been replaced by multielectrode 2D and 3D profiles. Portable field computers can now perform fast and sophisticated inversions on the fly. Electrical resistivity surveys are particularly good at detecting the features and subsurface changes associated with all types of karst (Torrese, 2020). Clay-filled fractures in limestone are detectable as low resistivity targets, while caves can be seen as high resistivity targets (Zhou et al., 2002). The resistivity change from an air or water filled passage next to a solid limestone block show up particularly well in surveys. The locations of each line in

this study were chosen to give the best coverage of the known cave passages as well as to avoid surface features unfavorable to electrical resistivity line placement. Electrical resistivity anomalies of fractures related to sinkholes can show up as low resistivities if the fractures are acting as hydraulic conductivity conduits (Ahmed and Carpenter, 2003). Air-filled cavities can show up in a survey with electrical resistivity reading in the tens of thousands while the surrounding solid subsurface can be anywhere between a few ohm-ms when wet up to the high hundreds to low thousands. Electric resistivity has been proven to be useful in detecting these high electrical resistivity anomalies (Peterson and Berg, 2001; Kaufmann et al., 2011; Land, 2011). ER is also useful in finding low electrical resistivity anomalies like ground water (Ezma et al., 2020). All electrical resistivity readings in karst environments are relative and the values measured in the same subsurface can change drastically from day to day and season to season depending on weather and subsurface conditions. Apparent electrical resistivity highs and lows are still reliable but specific values should be considered less important than relative high and low values.

ER Instrumentation. ER surveys were performed using the GF Instruments ARES Automatic Resistivity System (Figure 27) and the Supersting R8 (Figure 28). The ARES system uses a battery-powered computer, 8 multi-electrode cables, and 64 steel electrodes. The ARES computer is a programmable switch-box which automatically performs electrical resistivity surveys. The user must select a geometric array which includes electrode spacing and number of electrodes. The 8 multi-electrode cables each have 8 electrodes connected in sequence. These cables connect end to end to one another to create one long survey cable with 64 electrodes. This long cable is then connected to the ARES computer. Each electrode on the cable is fastened to

the steel stakes using rubber rings. The electrodes are inserted into the ground and must be solid and deep enough to provide a good electrical contact with the earth.



Figure 27. ARES system set up in the field



Figure 28. Supersting R8 set up in the field.

The Supersting R8 is an electrical resistivity system that consists of 4 smart cables with 14 electrode connections each, a gas generator powered computer, two power adapting boxes, one cable switch-box, and 56 steel electrodes with spring connectors. The smart cables and their corresponding electrodes are pre-fabricated with the exact electrode number in the sequence being predetermined. Electrode one must always be electrode one, electrode two must always be

electrode two, and so on and so forth. The smart cables connect end-to-end with the middle two cables connecting to the switch box in the middle of the line. Each electrode is connected to the smart cables using the spring connectors attached to each steel rod. The electrodes are inserted into the ground solid enough and deep enough to provide a good electrical connection with the earth. The user selects a pre-programmed array configuration on the Supersting R8 and the computer automatically performs the survey.

ER Data Collection. Once a survey is programmed and started both the ARES and Supersting R8 units systematically select current and potential electrode pairs to create a pseudosection of electrical resistivity points (Figure 29). This electrical resistivity data are stored in each computer's memory to be downloaded and processed by a computer in the lab. More than one survey can be conducted per trip on each system. Multiple surveys can be stored from multiple trips and saved indefinitely to be processed at a later date. With the ARES system a Schlumberger electrical resistivity survey will take about one and a half hours to complete using a 1-meter spacing and 64 electrodes and will collect around 990 data points. The Supersting R8 system will take around an hour to complete a dipole-dipole electrical resistivity survey using 1-meter spacing and 56 electrodes and will collect around 700 data points.

For this study, the typical configuration with both the ARES and Supersting R8 was to use all available electrodes. The spacing of each survey's electrode setup was heavily dependent on terrain. Typically, the spacing used was between 1 and 5 meters. A wider electrode spacing results in greater depth in the surveys observation, but with lower resolution. The Schlumberger and the dipole-dipole array were used for this thesis. The study area is in the woods away from roads and other forms of interference. The Schlumberger array was always used with the ARES system and the dipole-dipole system was always used with the Supersting R8. This decision was

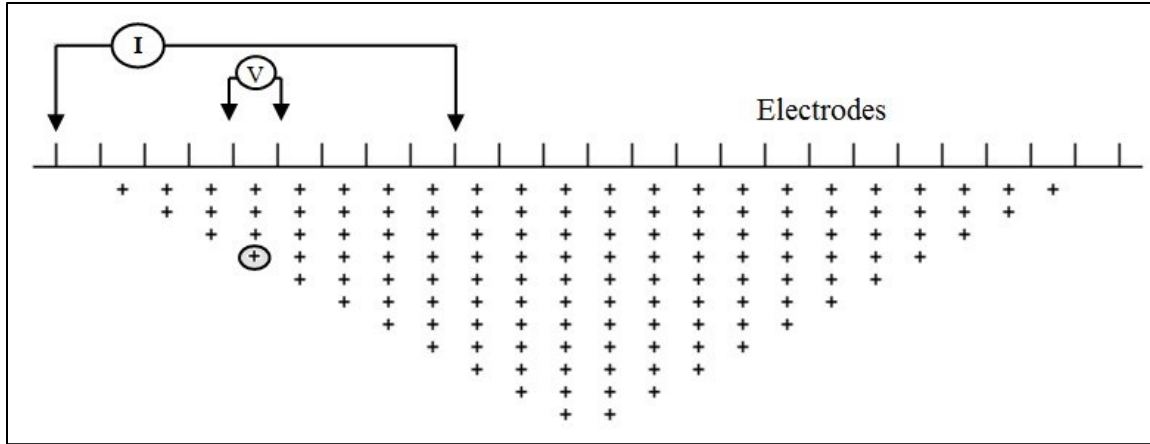


Figure 29. Data point distribution in a pseudosection from Schlumberger electrical resistivity array. Circled data point is a result of the illustrated current (I) and potential (V) electrode positions.

based simply on the best average survey times of each system. The ARES was programmed to take measurements four times for each point and average the results. The Supersting R8 was programmed to do two surveys for each line, one in the forward direction and one in the reverse direction.

The topography of the study area had a significant influence on the surveys. Generally, all the electrodes in a given line were not within the same elevation range of $\pm \frac{1}{2}$ of a meter. This means topography needed to be collected. An elevation was measured every ten meters along a line using a Reach RS2 GNSS Receiver (Figure 21).

Geospatial information for each survey was also collected using a GPS BLACK* device. Location of survey line endpoints, and any relevant features were all recorded typically with an accuracy of 0.5m.

ER Data Processing. Data from each survey was downloaded to a PC using GF Instruments software and converted into a format readable by AGI EarthImager 2D software. Electrical resistivity profiles were uploaded into AGI EarthImager 2D to view raw data and

perform a 2D inversion based on software by Loke (1999). The terrain files were included in the model. The software automatically removed anomalies like singular electrical resistivity spikes. For each set of survey data an inversion algorithm is run to produce an inverted electrical resistivity model from the measured apparent electrical resistivity pseudosection. This inversion was ran multiple times using robust inversion methods to determine which features of the model were required by the data.

RESULTS

Area 1 - Known Cave Under Large and Small Sinkholes

Area 1: Electrical Resistivity (ER). The ER surveys were performed to test the ability of ER to detect the known cave passages and to get a baseline reading to use in the discovery of new cave passages in the surrounding subsurface. Four west to east trending electrical resistivity lines were taken using the Schlumberger array (Figure 30).

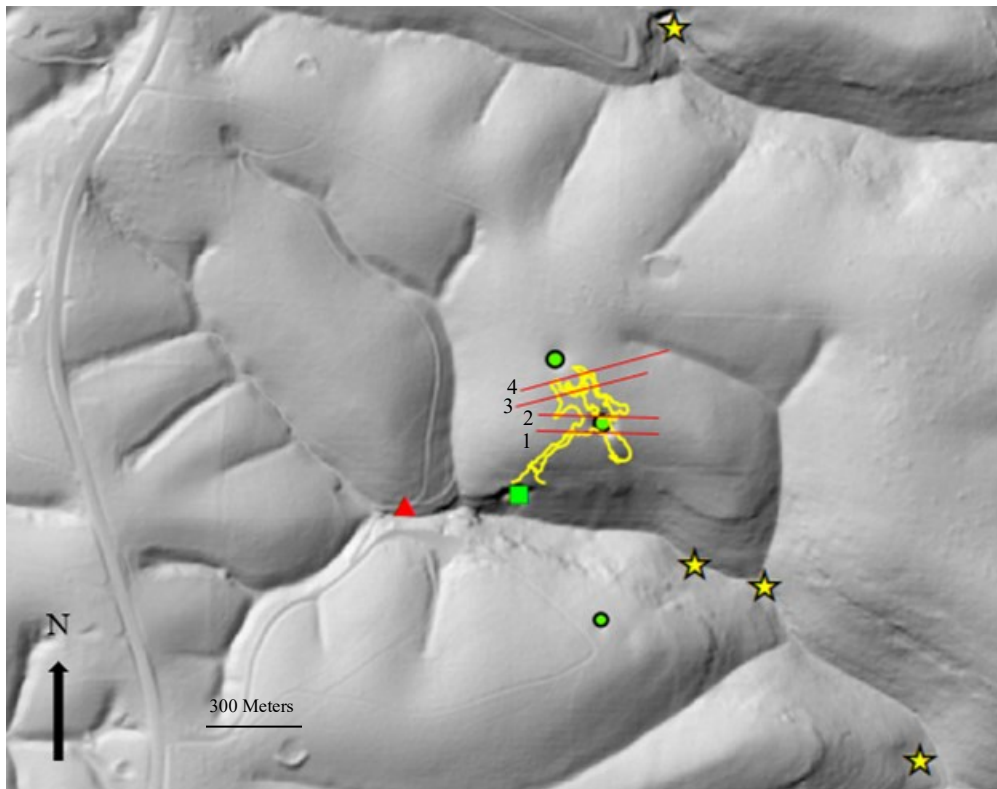


Figure 30. Hillshade showing the location of the four east to west trending lines 1 through 4 from area 1. Line 1 is the most southern line while line 4 is the most northern. The yellow outline is the cave map from Figure 5. Red triangles represent locations of small cave openings on the property. The green dots are the locations of sinkhole cones visible on the surface. The green square is the main cave entrance. The yellow stars are cave openings of interest.

Line 1 trends from east to west on the southern rim of the large sinkhole that is directly above the main cave chamber. The survey was conducted using the ARES system with an electrode spacing of 3m. The high electrical resistivity region (A) (1000 to 10000 ohm-m) that extends from the surface to the bottom of the profile corresponds to the location of the known cave and the sinkhole in the main chamber. The low electrical resistivity areas (B) (186 to 49.3 ohm-m) represent water saturated subsurface soil and rock (Figure 31).

Line 2 follows the same west to east trend but is situated on the northern rim of the large sinkhole above the known cave's main chamber. The high electrical resistivity region (A) (1000 to 2472 ohm-m) extends the full length of the profile from 15m to beyond 29.6m in depth corresponds to the expected location of the known cave chambers in the subsurface. The low electrical resistivity regions (B) (230 to 105 ohm-m) near the surface correspond to water saturated subsurface rocks and soil (Figure 32).

Line 3 trends from southwest to northeast and is situated near the midway point between the large and small sinkhole above the known cave location. The high electrical resistivity region (A) (1811 to 4956 ohm-m) that extends the length of the line from 20m to 29.8m in depth corresponds to the expected location of known cave passages in the subsurface. The low electrical resistivity regions (B) (242 to 88 ohm-m) represent water saturated subsurface rocks and soil (Figure 33).

Line 4 trends from the southwest to the northeast on the southern rim of the small sinkhole above the known cave. The two high electrical resistivity regions (A and B) (1735 to 4728 ohm-m) on either end of the profile correspond to two known chambers in the subsurface. This was slightly unexpected as the known cave map does not show the cave extending around the sinkhole location. This leaves an opportunity for lines to be taken around the sink hole to

confirm the new extent of the known cave or to discover possible unmapped cave passages. The relative low electrical resistivity values (1700 to 637 ohm-m) between the two highs corresponds

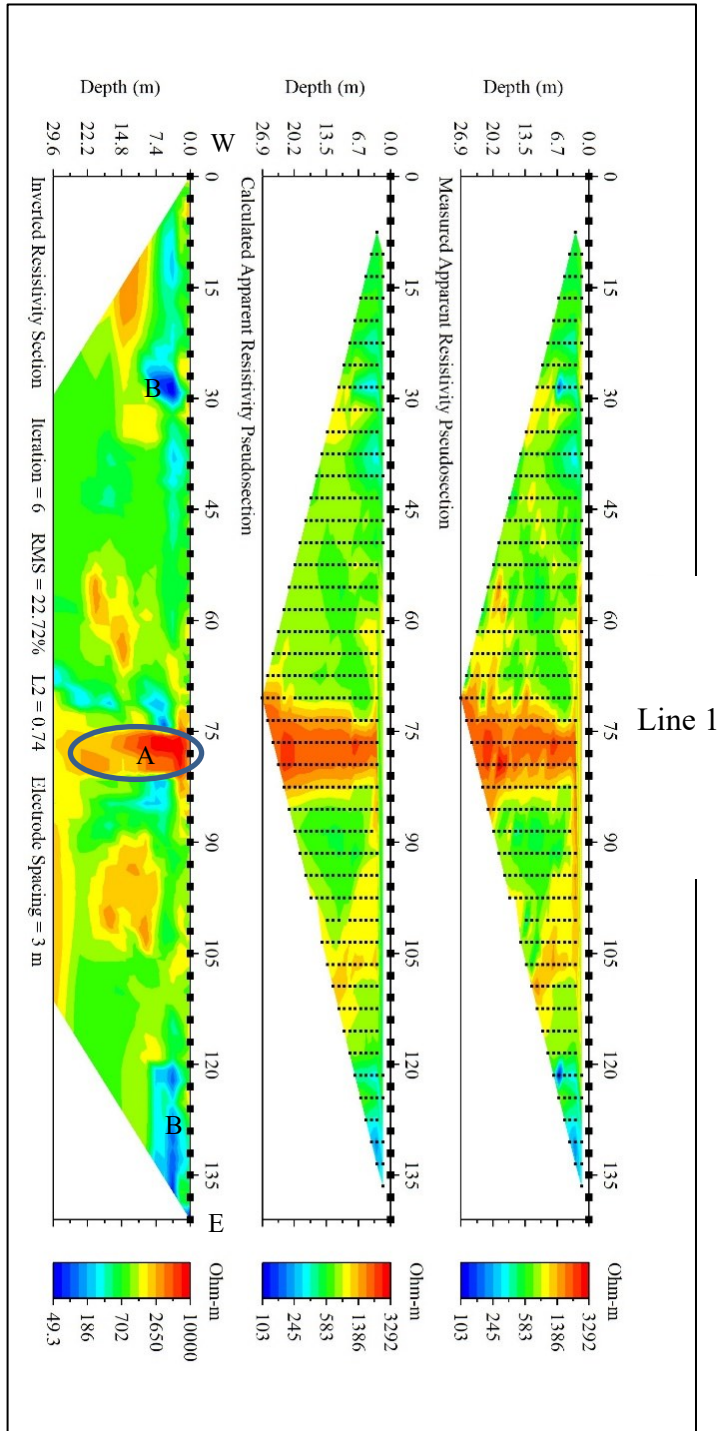


Figure 31. Measured apparent electrical resistivity, calculated electrical resistivity, and final electrical resistivity model for line 1 in area 1. A-the known cave, B-water saturated subsurface.

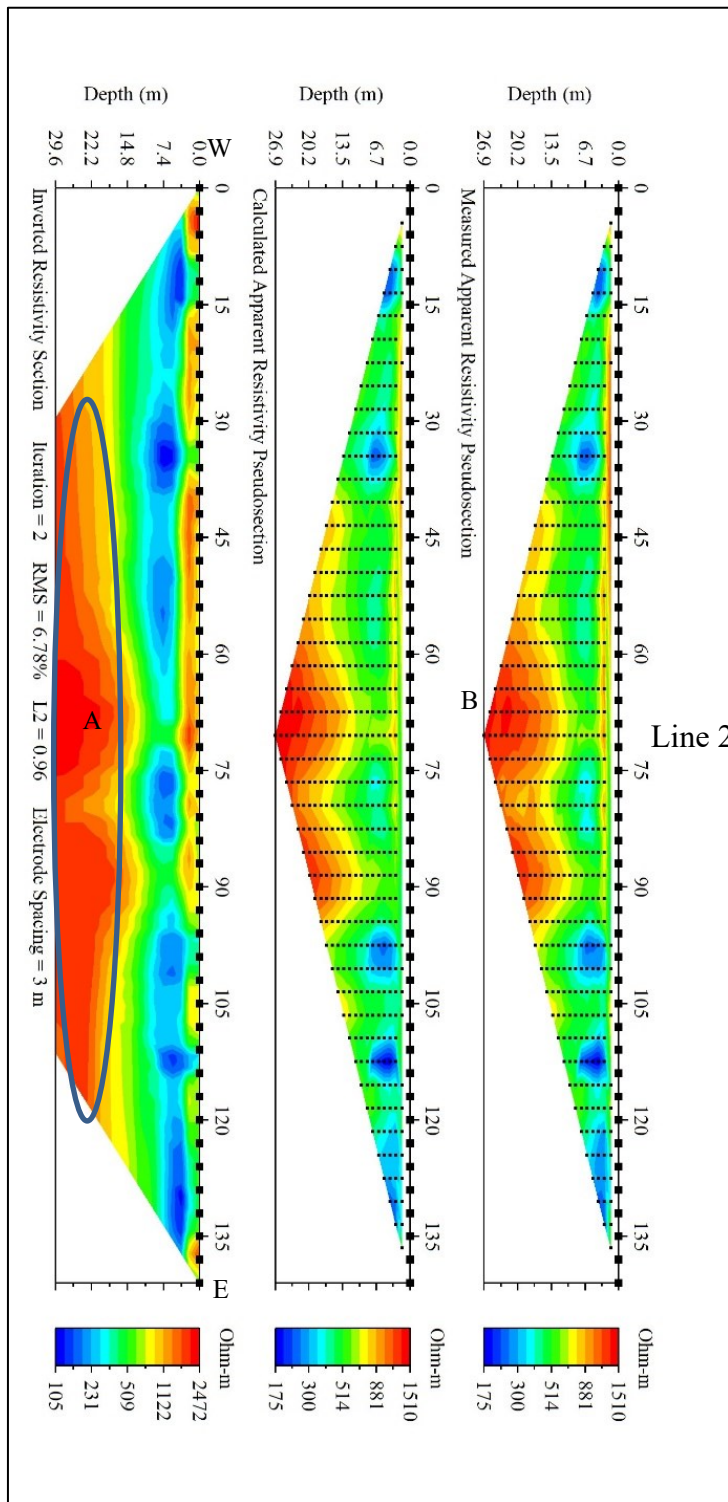


Figure 32. Measured apparent electrical resistivity, calculated electrical resistivity, and final electrical resistivity model for line 2 in area 1. A-the known cave, B-water saturated subsurface.

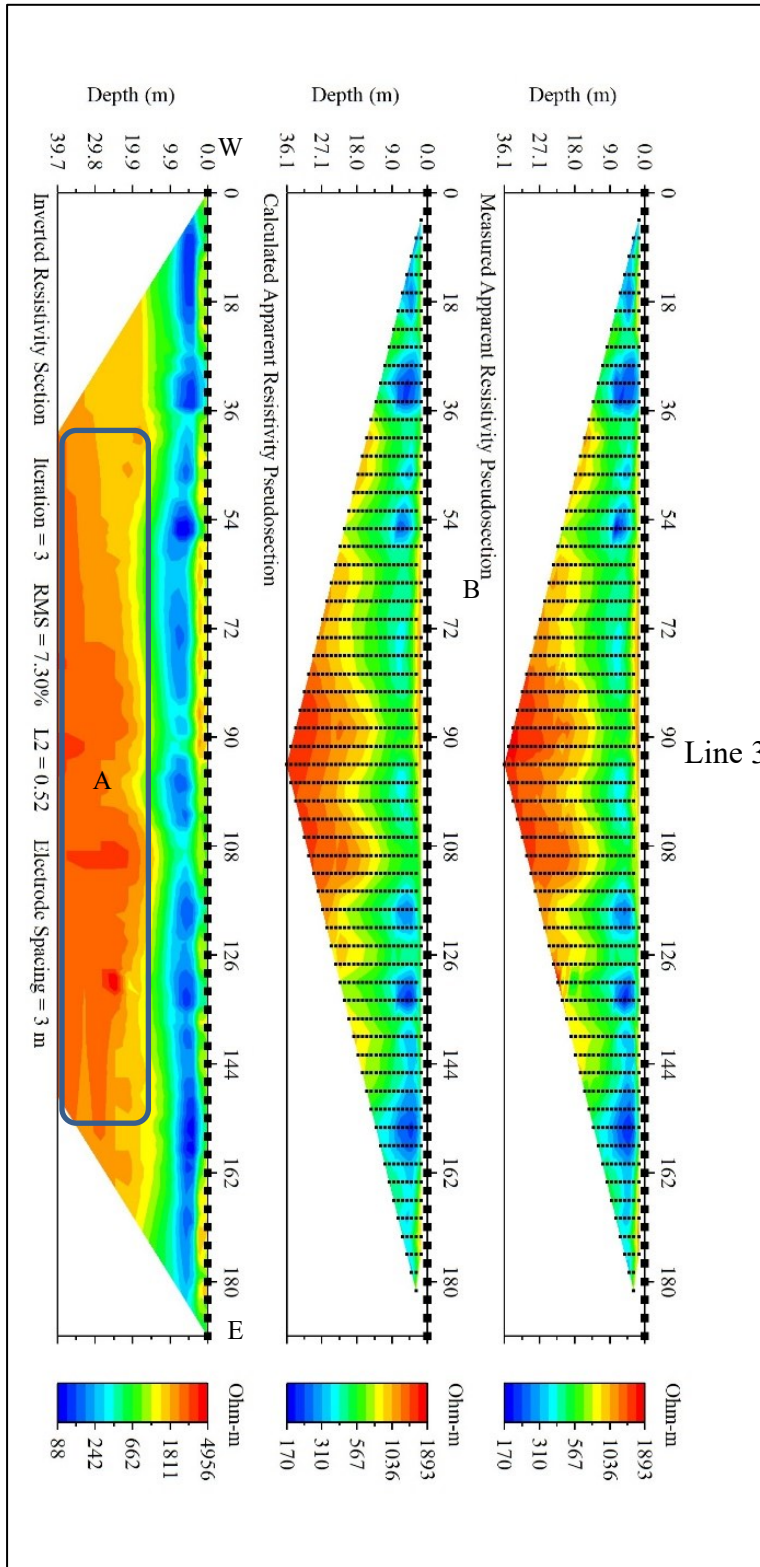


Figure 33. Measured apparent electrical resistivity, calculated electrical resistivity, and final electrical resistivity model for line 3 in area 1. Circled A-the known cave, B-water saturated subsurface.

to the breakdown and debris (C) within the known cave passage. The low electrical resistivity areas (234 to 86 Ohm-m) represent water saturated subsurface rocks and soil (Figure 34).

The electrical resistivity profiles obtained in this area successfully served their purpose. The surveys confirmed the viability of using ER exploration in this specific type of southwest Missouri karst. The surveys confirmed the location of known subsurface voids and the values obtained will be used as relative base values for exploration in the unknown areas surrounding the cave.

Area 2 – Long Crawl Cave

Area 2: Electrical Resistivity (ER). The electrical resistivity surveys conducted here were performed to see if a connection between the study area and the long crawl cave across the local highway 1 kilometer away could be found. The area selected to be tested was chosen because it lays directly between the main chamber of the cave and the direction the long crawl cave trends. The area is also easy to access as it is along the sides of a local road. Both caves lay at an elevation of about 350m above sea level so two electrical resistivity lines (Figure 35) long enough to record data at that depth were taken. Both lines in this area were taken with the ARES system using the Schlumberger array.

Line 5 is located on the east side of the road and trends from south to north. The line was conducted with an electrode spacing of 3m. The line shows a trend from a low (B) (63 ohm-m) electrical resistivity to a high (A) (1014 ohm-m) electrical resistivity that is mostly uniform over the length of the line. This trend seems to not suggest the presence of a void and rather a relatively homogenous subsurface that decreases in conductivity with depth. The line was taken

during the dry season and the relative high electrical resistivity reading at the bottom is due to dry solid subsurface conducting electricity less readily than subsurface that is saturated (Figure 36).

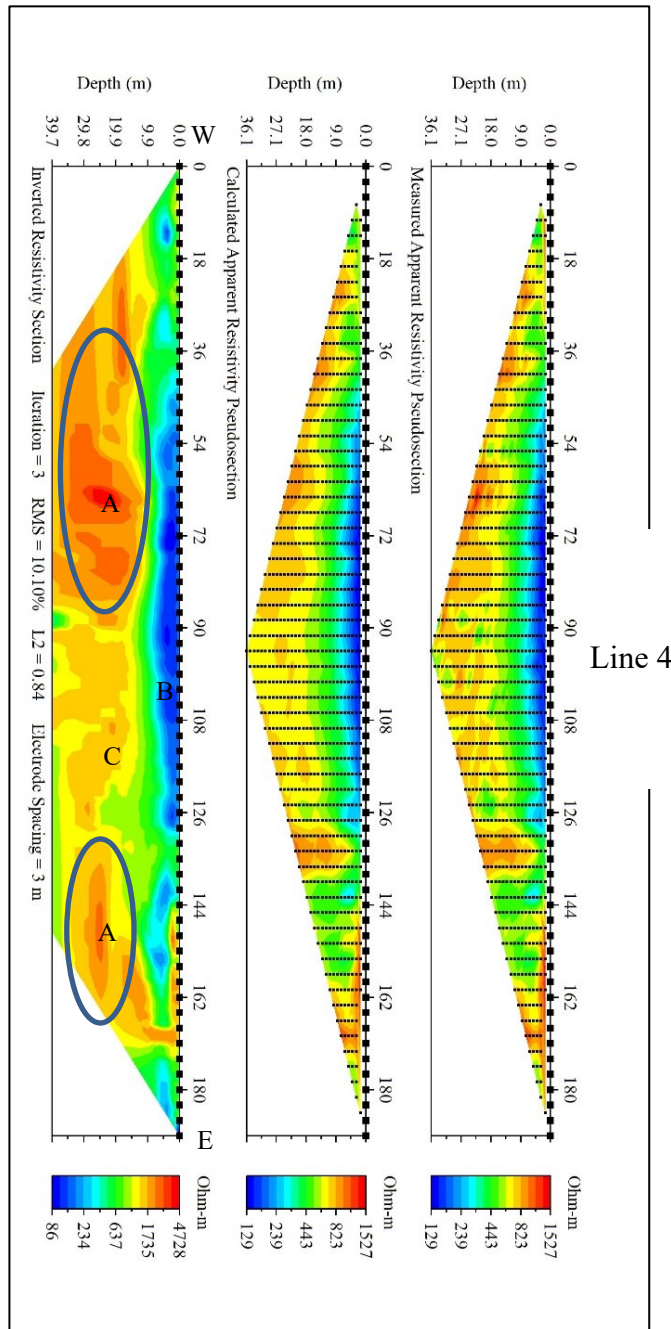


Figure 34. Measured apparent electrical resistivity, calculated electrical resistivity, and final electrical resistivity model for line 4 in area 1. Circled A-the known cave, B-water saturated subsurface, C-breakdown and debris.

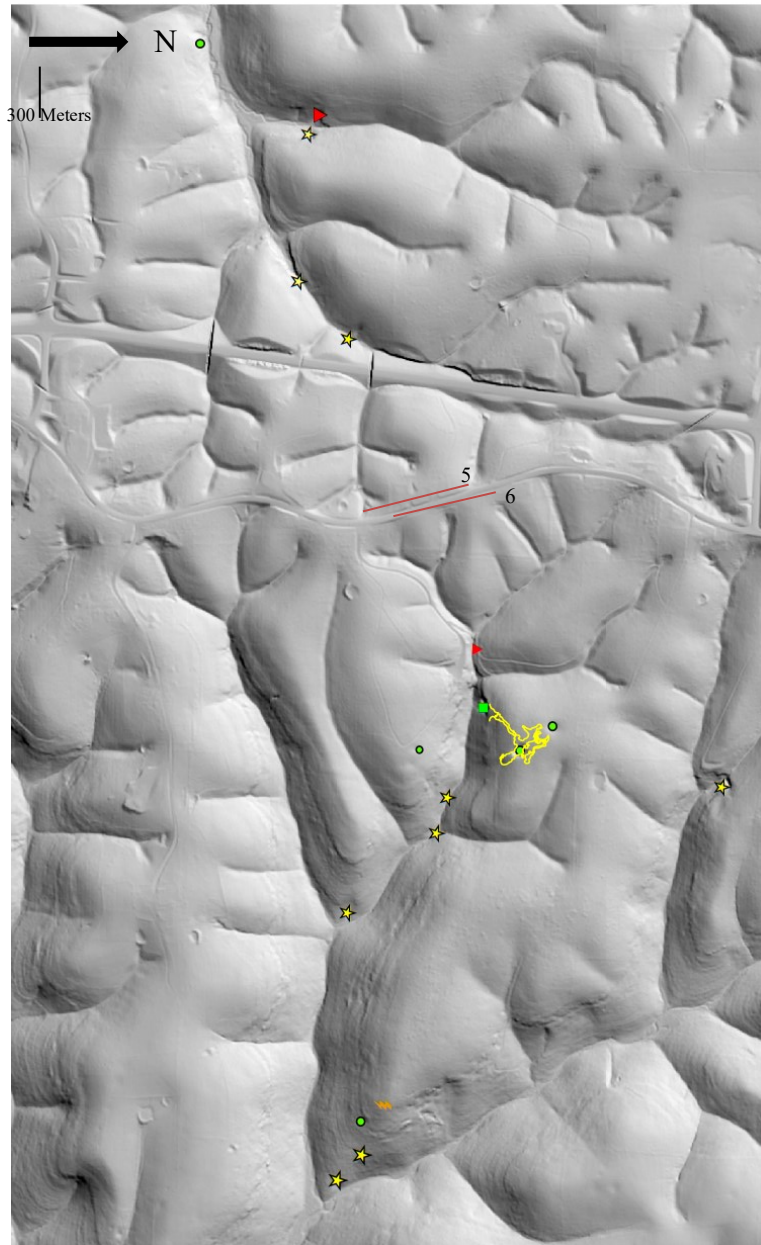


Figure 35. Hillshade showing the location of electrical resistivity lines 5 and 6 in red. The yellow outline is the cave map from Figure 5. Red triangles represent locations of small cave openings on the property. The green dots are the locations of sinkhole cones visible on the surface. The green square is the main cave entrance. The yellow stars are cave openings of interest. The brown lightning bolt is a powerline tower.

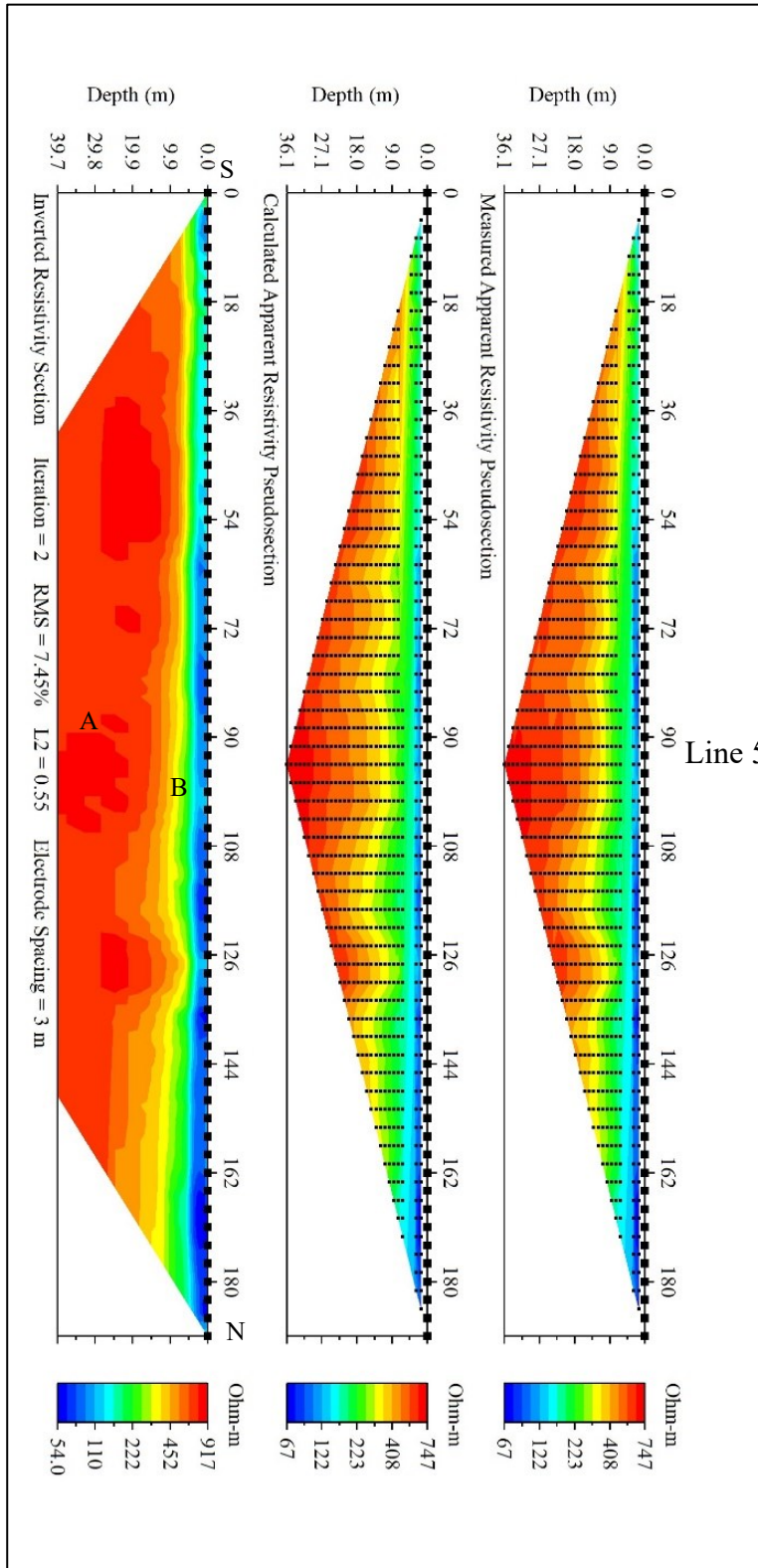


Figure 36. Measured apparent electrical resistivity, calculated electrical resistivity, and final electrical resistivity model for line 5 in area 2. A-drier subsurface, B-more saturated subsurface.

Line 6 in this area is located on the west side of the road and trends from south to north. The line was taken with a 3 m electrode spacing. The line shows a trend from a low (B) (67 ohm-m) electrical resistivity to a high (A) (917 ohm-m) electrical resistivity that is mostly uniform over the length of the line. This trend seems to not suggest the presence of a void and rather a relatively homogenous subsurface that decreases in conductivity with depth. The line was taken during the dry season and the relative high electrical resistivity reading at the bottom is due to dry solid subsurface conducting electricity less readily than subsurface that is saturated (Figure 37).

The models in this area cannot conclusively say if a subsurface void exists that connects the long crawl cave to the main cave. More data is needed to say this for certain. However, for this study the data were deemed enough to decide that other areas should become the focus for further electrical resistivity profiles.

Area 3 – East of Main Cave and Large Sinkhole

Area 3: Electrical Resistivity (ER). The electrical resistivity surveys at this location were performed to try to detect possible undiscovered voids in the subsurface directly to the east of the known cave. Any voids detected in this area would be close enough to the known cave that a connection between the two would be likely. The electrical resistivity lines in this area were taken with both the ARES unit using the Schlumberger array and the Supersting R8 using the dipole-dipole array. This location was selected because a spring to the southeast of the known cave has water that flows out of it that could possibly be from a stream that runs through the known cave. The lines taken here had to be moved further north than originally wanted because

of the cliff to the south of the cave. The slope to the cliffs edge proved to be steeper than the known cave and spring (Figure 38).

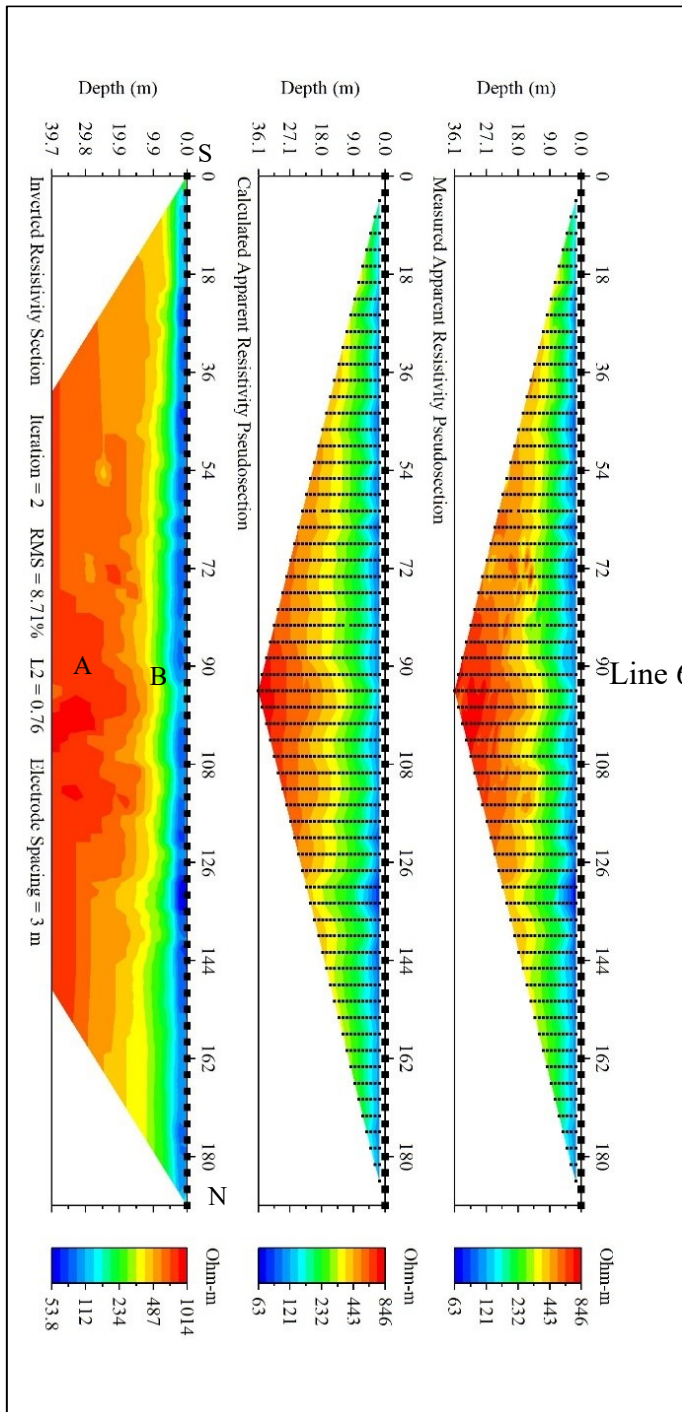


Figure 37. Measured apparent electrical resistivity, calculated electrical resistivity, and final electrical resistivity model for line 6 in area 2. A-drier subsurface, B-more saturated subsurface. expected and the lines were unable to be placed far enough south to detect connections between

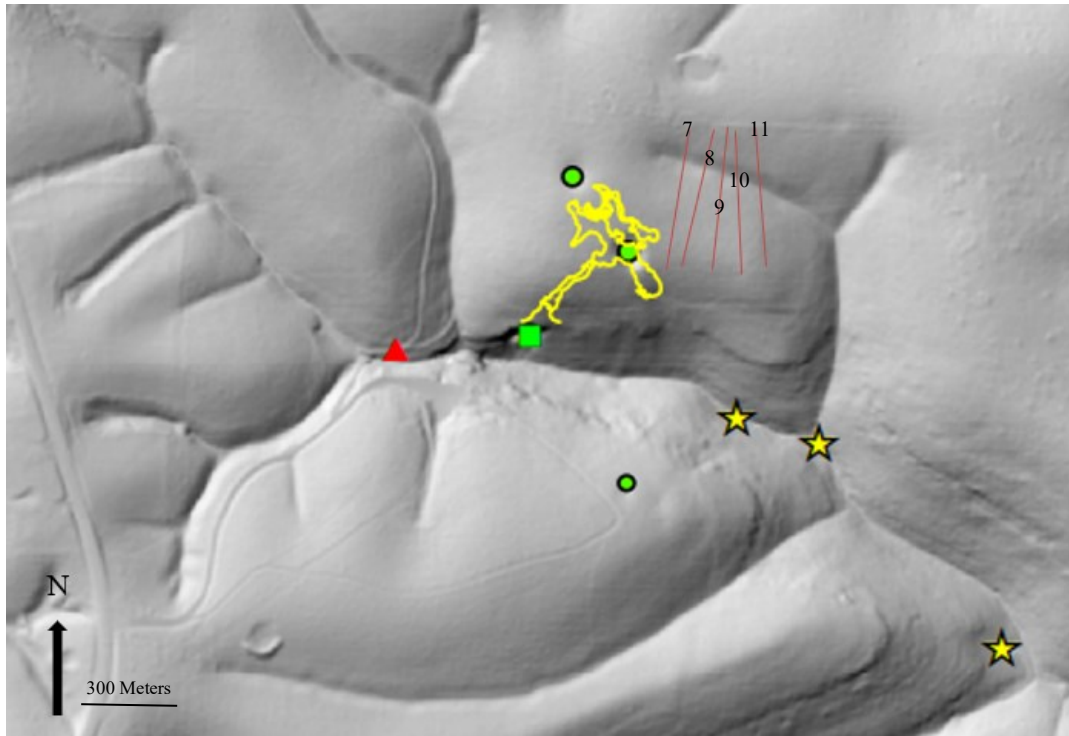


Figure 38. Map showing the location of study area 3. Lines shown are lines 7-11 from left to right. The yellow outline is the cave map from Figure 5. Red triangle represent location of small cave opening on the property. The green dots are the locations of sinkhole cones visible on the surface. The green square is the main cave entrance. The yellow stars are cave openings of interest.

Line 7 was collected using the ARES unit with an electrode spacing of 2 m. The line is east of the large sinkhole and trends from north to south. The high (5,000 to 28,989 Ohm-m) electrical resistivity region (A) is consistent with the expected readings of an undetected void in the subsurface for this area. The region is at an elevation (380m to 360m) that is consistent with the depth of the known cave passages (Figure 39).

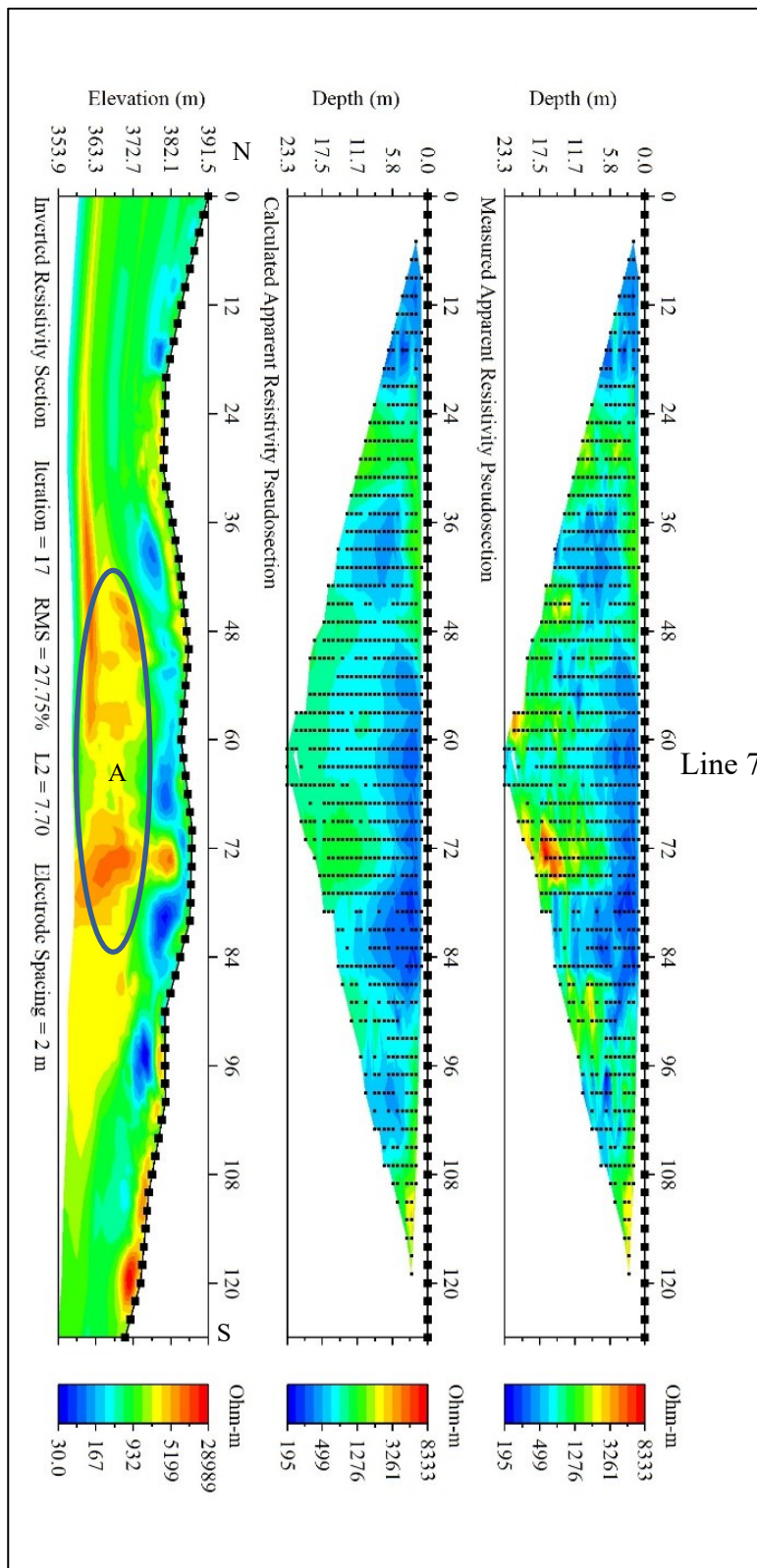


Figure 39. Measured apparent electrical resistivity, calculated electrical resistivity, and final electrical resistivity model for line 7 in area 3. Circled A-subsurface void.

Line 8 was collected using the ARES unit with an electrode spacing of 2 m. The line is east of line 7 and trends from north to south. The high (4,000 to 77,369 ohm-m) electrical resistivity region (A) is consistent with the expected readings of an undetected void in the subsurface for this area. The region is at an elevation (376m to 360m) that is consistent with the depth of the known cave passages (Figure 40).

Line 9 was collected using the Supersting R8 unit with an electrode spacing of 3 m. The line is in the middle of the other four lines, between the detected high resistivities and trends from the north to the south. The high (2,800 to 8,906 ohm-m) electrical resistivity region (A) in the left part of the line is consistent with the expected readings of an undetected void in the subsurface for this area. The high (about 2,000 to 6,000 ohm-m) electrical resistivity region in the right part of the line is consistent with the expected readings of an undetected void in the subsurface for this area. The high electrical resistivity is at an elevation (370m to 360m) that is consistent with the depth of the known cave passages (Figure 41).

Line 10 was collected using the ARES unit with an electrode spacing of 2 m. The line is east of line 2 and trends from north to south. The high (5,758 to 29,920 ohm-m) electrical resistivity regions (A) in the right and left portions of the line is consistent with the expected readings of an undetected void in the subsurface for this area. The regions are at an elevation (375m to 360m) that is consistent with the depth of the known cave passages (Figure 42).

Line 11 was collected using the ARES unit with an electrode spacing of 2 m. The line is east of line 3 and trends from north to south. The high (4,799 to 15,684 ohm-m) electrical resistivity region (A) in the left part of the line is consistent with the expected readings of an undetected void in the subsurface for this area. The high (about 2,000 to 5,000 ohm-m) electrical resistivity region in the right part of the line is consistent with the expected readings of an undetected void

in the subsurface for this area. The high resistivities are at an elevation (370m to 360m) that is consistent with the depth of the known cave passages (Figure 43).

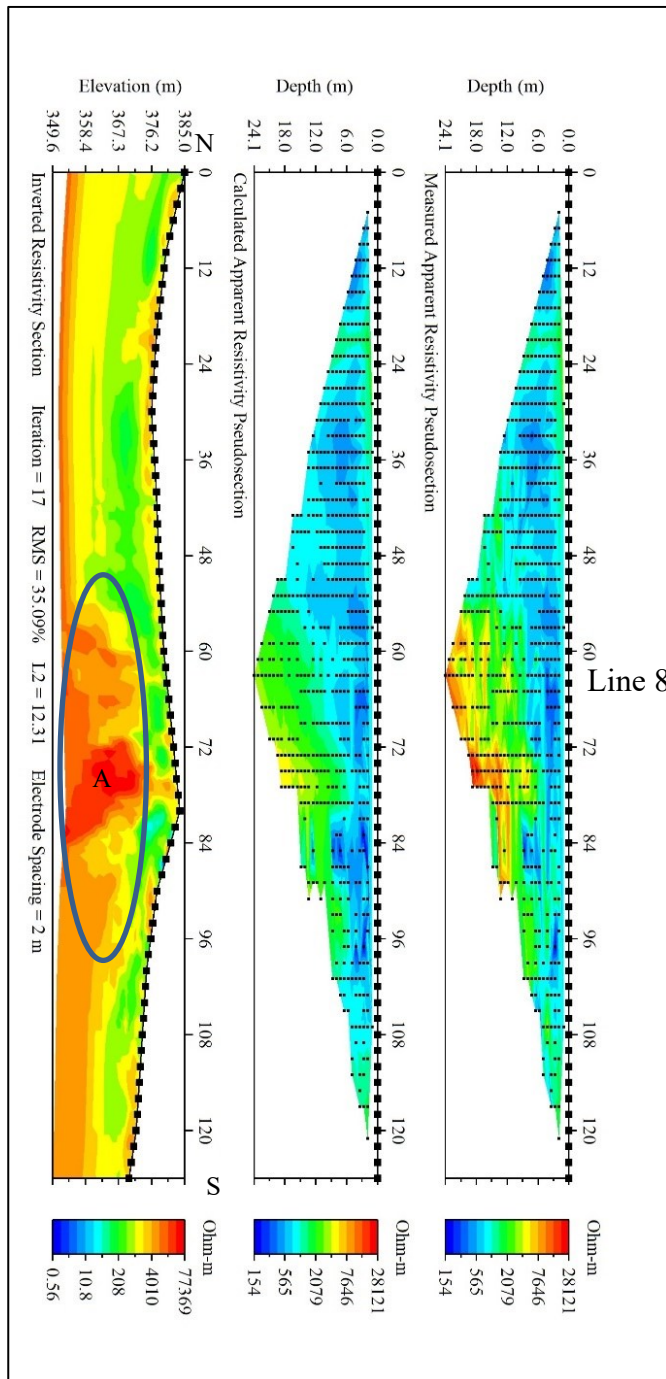


Figure 40. Measured apparent electrical resistivity, calculated electrical resistivity, and final electrical resistivity model for line 8 in area 3. Circled A-subsurface void.

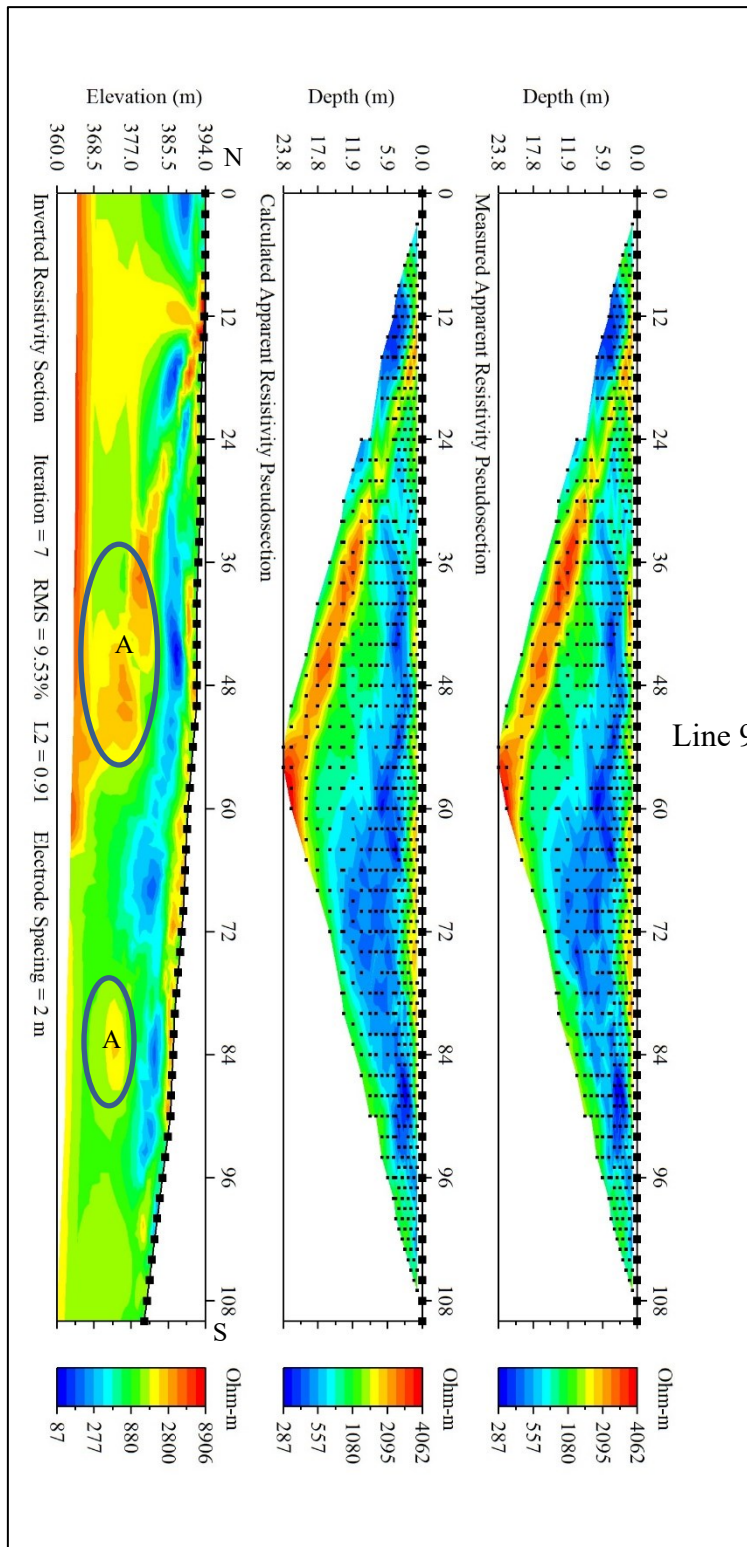


Figure 41. Measured apparent electrical resistivity, calculated electrical resistivity, and final electrical resistivity model for line 11 in area 3. Circled A-subsurface void.

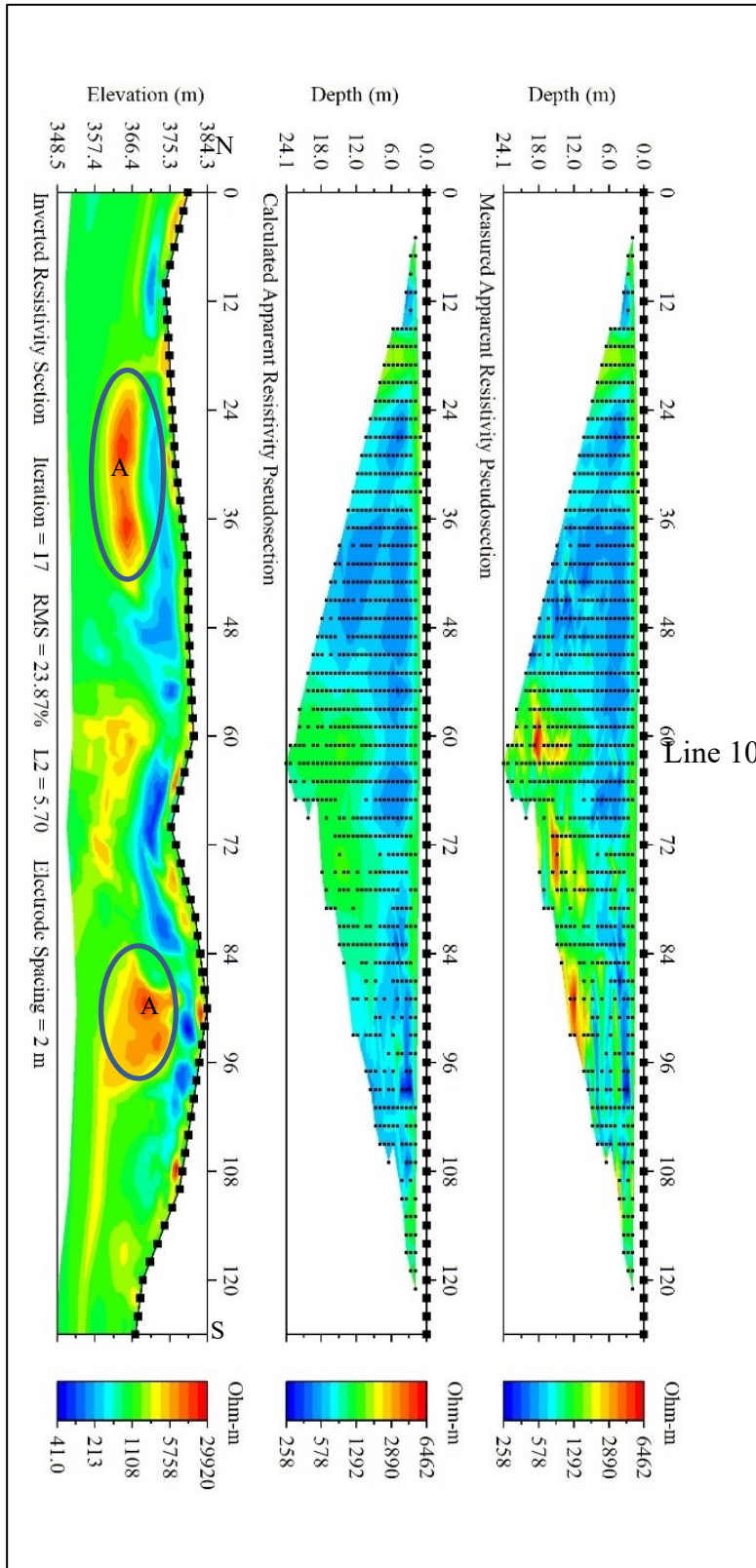


Figure 42. Measured apparent electrical resistivity, calculated electrical resistivity, and final electrical resistivity model for line 9 in area 3. Circled A-subsurface void.

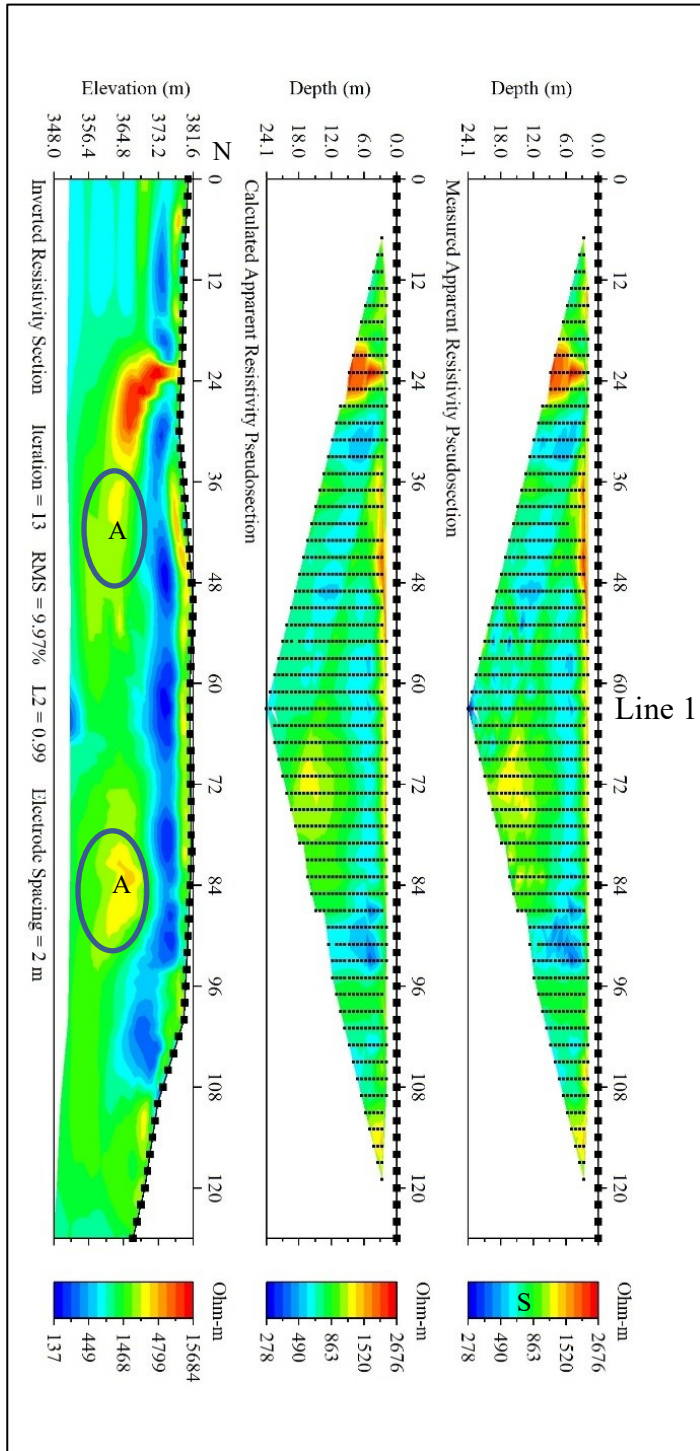


Figure 43. Measured apparent electrical resistivity, calculated electrical resistivity, and final electrical resistivity model for line 10 in area 3. Circled A-subsurface void.

The data collected seem to suggest the existence of a large void in the subsurface that lies to the northeast of the large main cave chamber. The void appears to trend from the northwest to the southeast and takes up much of the subsurface in the western part of the study area. Excavation is required to confirm this conclusion and to find a possible connection between this void and the known cave.

Area 4 – Small Sinkhole Northwest of Main Cave Chamber

Site 1: Electrical Resistivity (ER). The surveys at this location were performed to try to detect possible undiscovered voids in the subsurface directly to the east of the known cave. Any voids detected in this area would be close enough to the known cave that a connection between the two would be likely. The electrical resistivity lines in this area were taken with both the ARES unit using the Schlumberger array and the Supersting R8 using the dipole-dipole array. This location was selected because the small sinkhole to the northeast of the main large sinkhole corresponds with breakdown within the cave that covers a large portion of the inside of the cave. This breakdown nearly obstructs entrance into a large portion of the cave to the north. It also covers a large enough portion of the caves floor and wall to the east that it may be obstructing entrance into a lost void in the subsurface (Figure 44).

Line 12 was collected with the ARES unit with an electrode spacing of 2 m. The line lays on the eastern side of the small sinkhole and trends from the north to the south. The line contains two high (up to 10277 ohm-m) electrical resistivity regions (A) at about 380m to 369m (Figure 45). This location is consistent with what would be expected from a void that is obstructed by the breakdown debris within the cave associated with the small sinkhole (Figure 13).

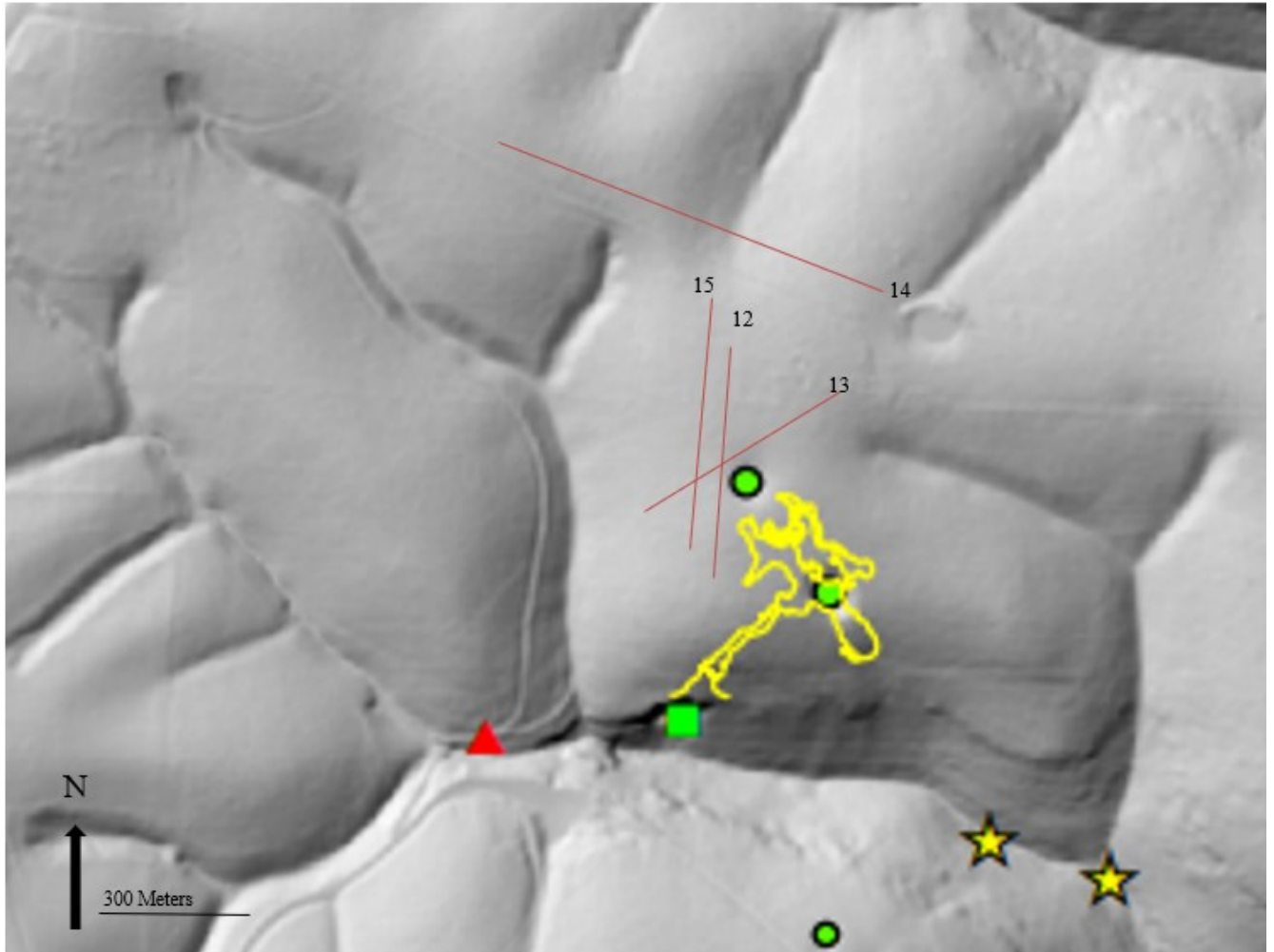


Figure 44. Map showing the location of study area 4. Lines shown are lines 12-15 from left to right. The yellow outline is the cave map from Figure 5. Red triangle represents location of small cave opening on the property. The green dots are the locations of sinkhole cones visible on the surface. The green square is the main cave entrance. The yellow stars are cave openings of interest.

Line 13 was collected using the Supersting R8 with an electrode spacing of 3 m. It is located 5 m to the west of line 12 and trends from the north to the south. The high (2,013 to 7,101 ohm-m) electrical resistivity region (A) in the right part of the line is consistent with the expected readings of an undetected void in the subsurface for this area. The high electrical resistivity area is at an elevation (370m to 360m) that is consistent with the depth of the known cave passages (Figure 46).

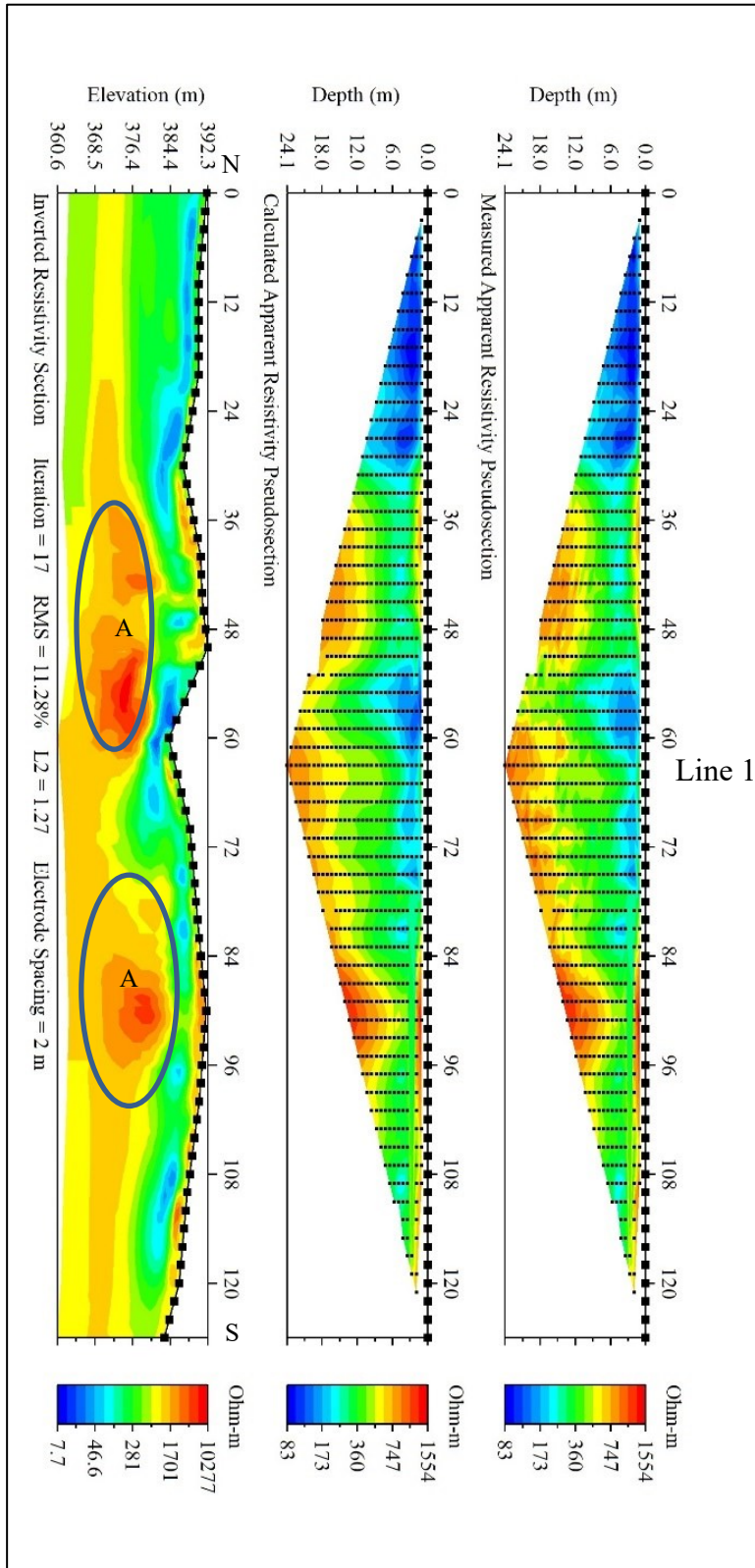


Figure 45. Measured apparent electrical resistivity, calculated electrical resistivity, and final electrical resistivity model for line 12 in area 4. Circled A-subsurface void.

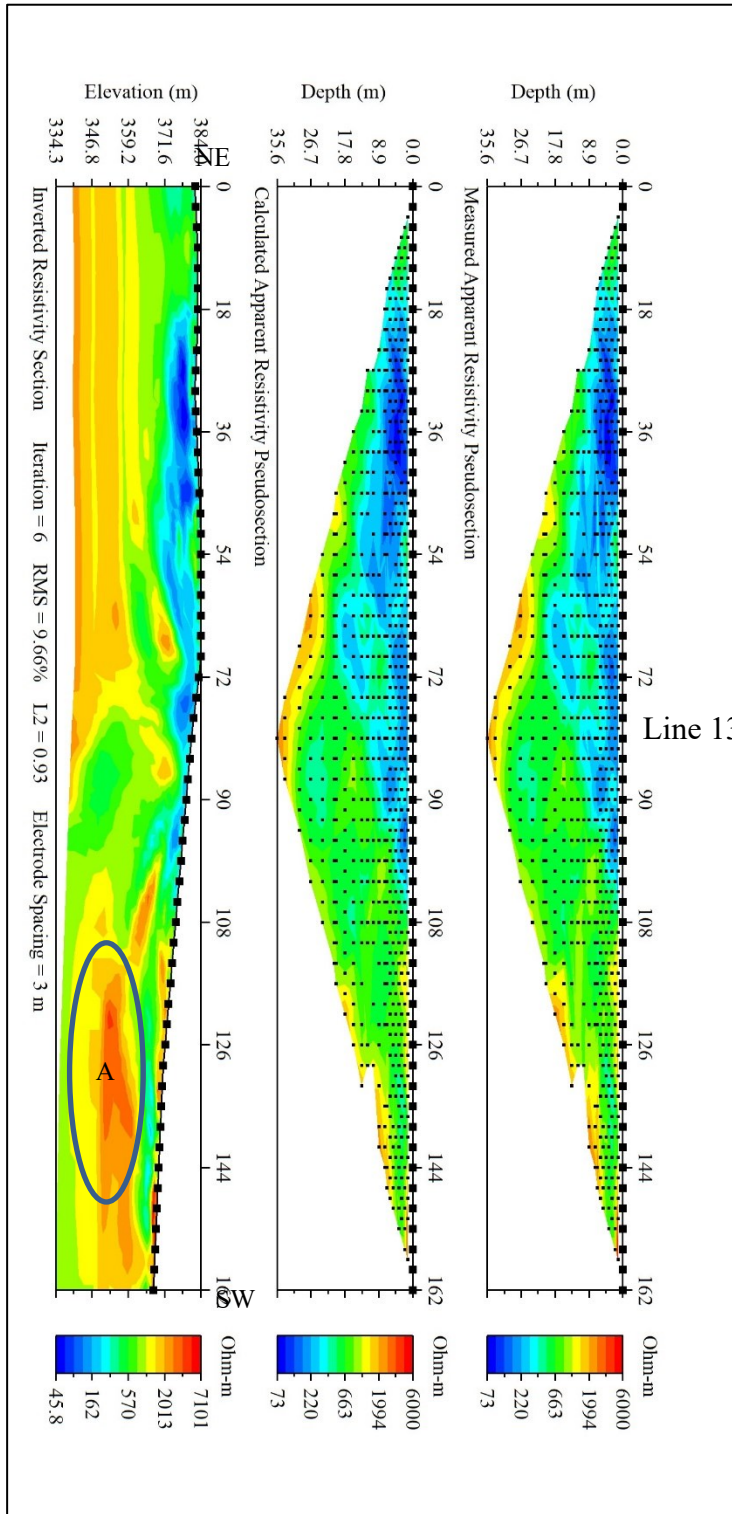


Figure 46. Measured apparent electrical resistivity, calculated electrical resistivity, and final electrical resistivity model for line 12 in area 4. A-subsurface void.

Line 14 is located further to the north along an access road to the study location. This line was collected using the Supersting R8 with an electrode spacing of 5 m. This line was taken to try to detect any voids in the subsurface that may extend out of the study area to the north. The land north of the study area belongs to an unknown person and access to the land was not obtained. The high (2,145 to 8,198 ohm-m) electrical resistivity region (A) in the center part of the line is consistent with the expected readings of an undetected void in the subsurface for this area. (Figure 47).

Line 15 is located west of line 12. This line was collected using the Supersting R8 with an electrode spacing of 3 m. This line was taken to try to detect any voids in the subsurface that may extend past the small sinkhole beyond line 12. The high (1,942 to 6,316 ohm-m) electrical resistivity region (A) in the right part of the line is consistent with the expected readings of an undetected void in the subsurface for this area. (Figure 48).

The data collected in this area seems to suggest the existence of a cave passage to the west of the known cave. The entrance to this void space in the subsurface is hidden by breakdown if it exists. Excavation is required to confirm or deny the existence of this void and its possible connection to the known cave.

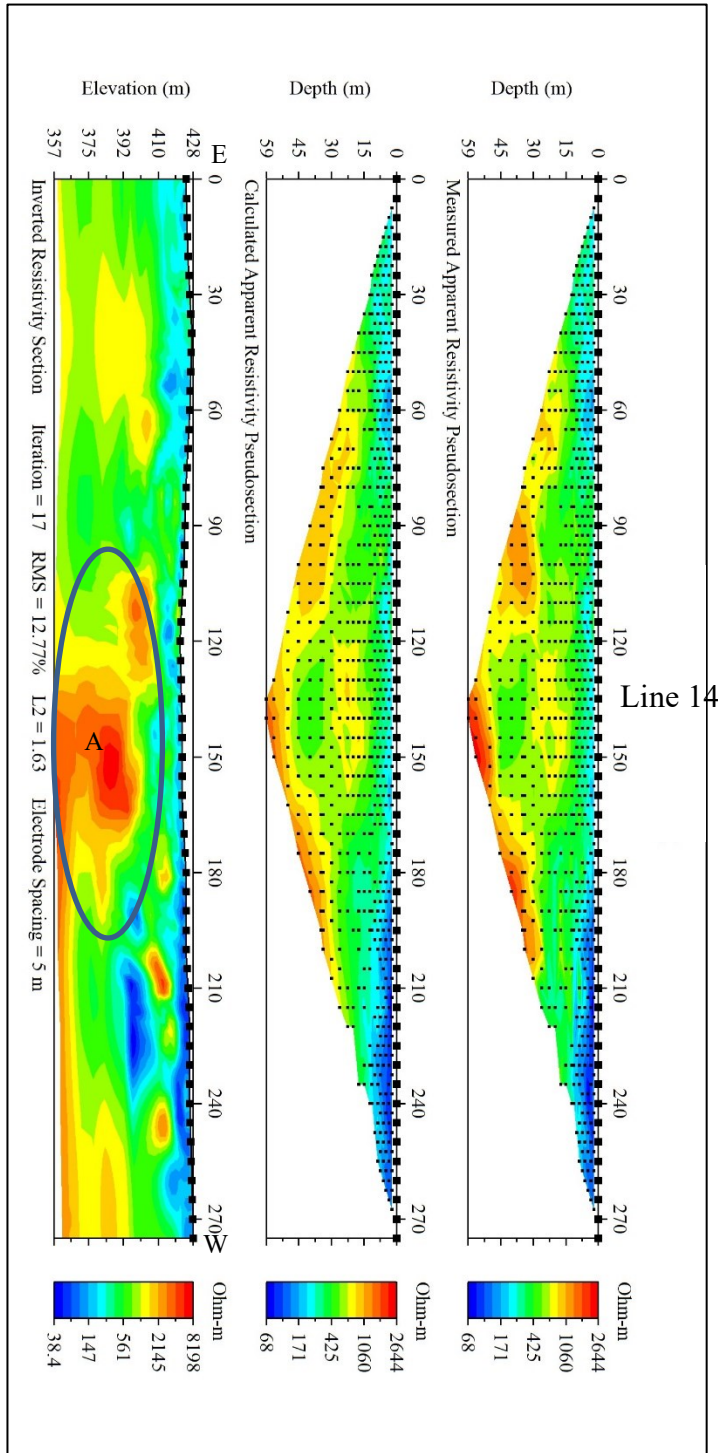


Figure 47. Measured apparent electrical resistivity, calculated electrical resistivity, and final electrical resistivity model for line 12 in area 4. A-subsurface void.

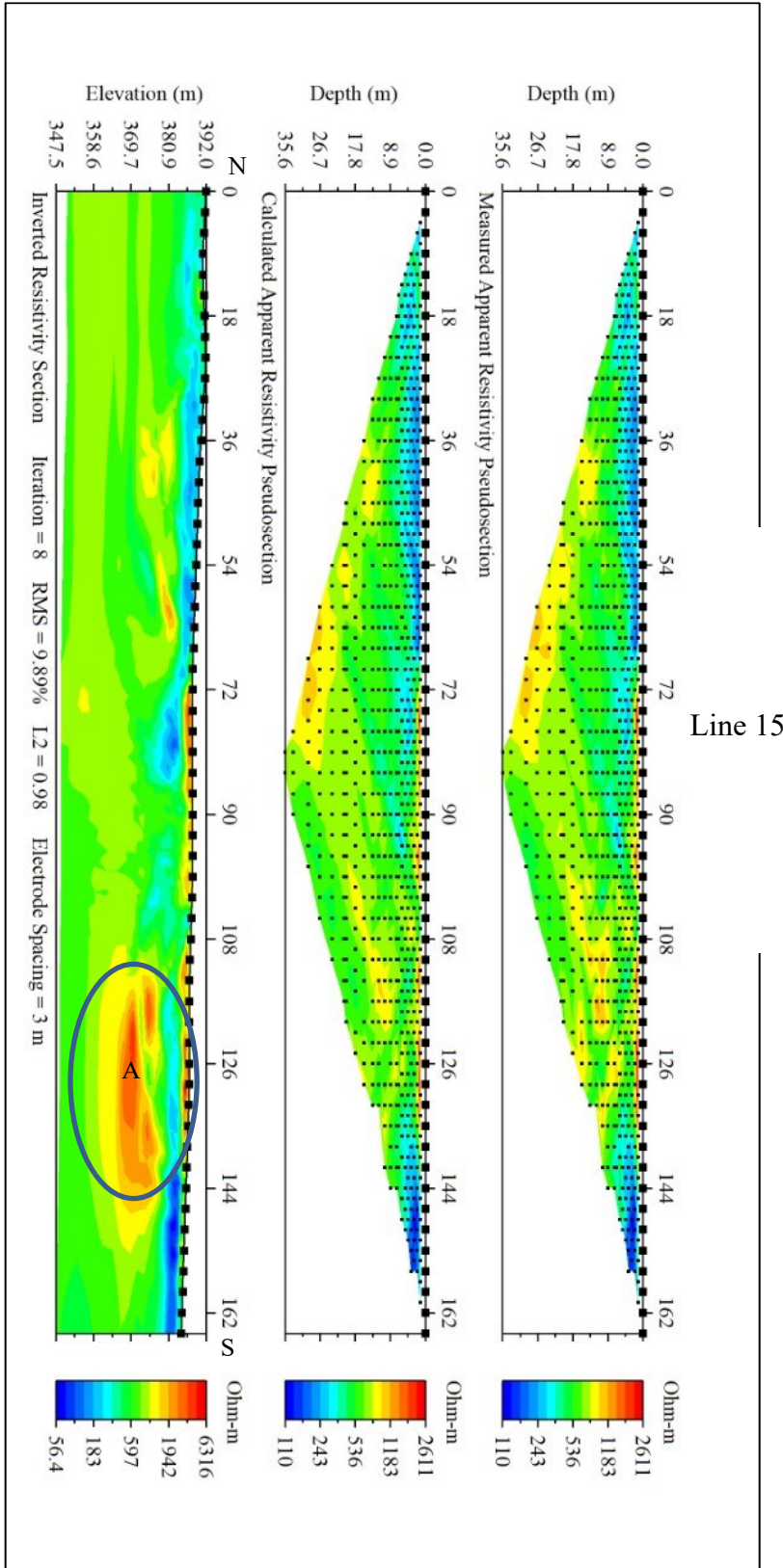


Figure 48. Measured apparent electrical resistivity, calculated electrical resistivity, and final electrical resistivity model for line 12 in area 4. A-subsurface void.

DISCUSSION

The trends of known karst features like fractures and sinkholes were successfully used as an indicator for finding voids in the unexplored subsurface (Figure 49). Some of the most promising data were collected in an area with few karst features to determine the extent of these features. Electrical resistivity data have been examined and interpreted in order to make the most accurate predictions possible for the locations of the new subsurface voids and sinkholes.

Some areas around the cave, like area 2 (Figure 35), had karst features that seemed promising before electrical resistivity was utilized. The depth and subsurface trend of Long Crawl Cave made it a promising candidate, but the investigation returned data and models (Figures 35-37) that indicated no presence of a subsurface void of a reasonable size that would connect Long Crawl Cave with Old Spanish Cave. Instead, the relatively high electrical resistivity portions of the model (Figures 36 and 37) only indicated moisture changes in the subsurface rather than structural changes.

Other areas, like area 4 (Figure 44) near the small sinkhole (Figure 13), had surface features that alluded to the presence of a subsurface void and produced electrical resistivity models that confirmed the presence of voids (Figures 45-48). The branches around both sides of the mapped cave would lead one to believe that the cave continues past the sinkhole. The models indicate two high electrical resistivity bodies that indicate the branches may continue past the sinkhole but are being blocked by breakdown. The northern branch may also extend up beyond the boundaries of the study area, but more data would be required to say for sure whether or not the two voids connect.

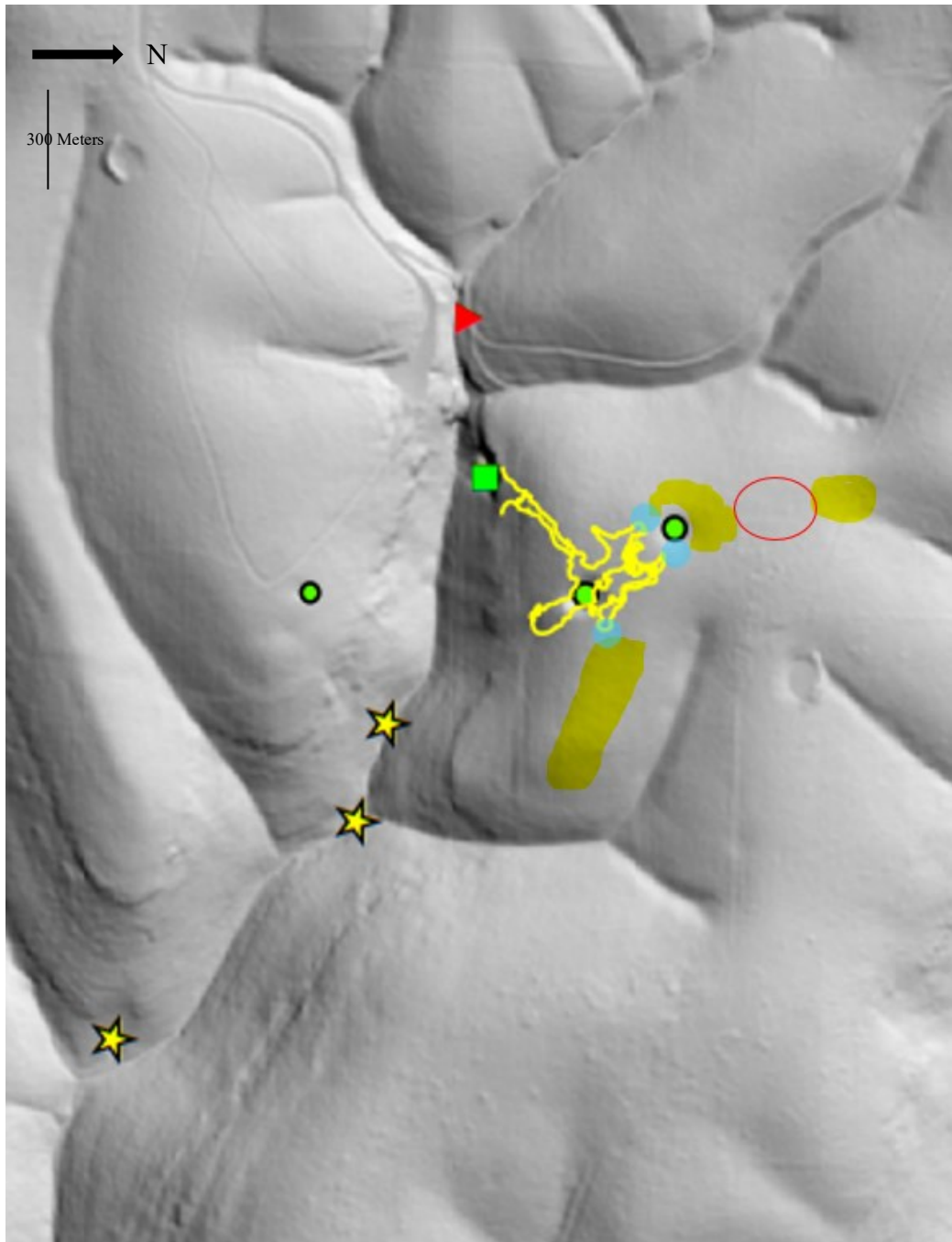


Figure 49. Map showing the known cave outlined in yellow. The yellow highlighted areas are the interpreted locations of subsurface voids detected by electrical resistivity survey. The blue highlighted areas represent places where connections between the known cave and the newly detected cave passages may exist. The red circle is an area where more data is needed to determine whether the northern most void connects to the rest of the cave system or not. The yellow outline is the cave map from Figure 5. Red triangles represent locations of small cave openings on the property. The green dots are the locations of sinkhole cones visible on the surface. The green square is the main cave entrance. The yellow stars are cave openings of interest.

While using the known karst features to constrain the investigation is a helpful way to search for subsurface voids, some subsurface features do not have a surficial presence. The surface above area 3 (Figure 38) was devoid of the type of obvious features which would indicate the presence of a large subsurface void. The electrical resistivity models (Figures 39-43) indicated the best candidate for a subsurface void that could expand the dimensions of the known cave. The highly electrical resistive area that appears to exist in this subsurface could be nearly 70 m long, up to 20 m wide, and within just a few meters of the known cave. If a void large enough for a human to pass through exists in this short distance and is blocked due to large breakdown, the large void could be excavated and explored. This would greatly increase the size of the cave and add on the largest chamber to be discovered thus far. This map (Figure 49) shows the possible extent of these new cave passages.

While southwest Missouri karst features do not necessarily directly correlate to karst features in all karst environments, the data collected and examined in this study suggest that karst exploration can be helped by using known features to determine the location of possible hidden features. Methods such as electrical resistivity are extremely useful when it comes to investigating karst subsurface. This method provides quantitative data rather than an estimation of what is happening in the subsurface based on visible features. Electrical resistivity is also non-invasive, easy to use, and is applicable to a variety of karst environments. This makes it an ideal candidate for other studies involving sinkholes and cave formations.

CONCLUSIONS

An electrical resistivity survey was conducted in southwest Missouri to determine the extent of known cave passages and estimate where additional cave passages in the same area around that known cave might exist. Fifteen two-dimensional profiles were collected using the dipole-dipole and Schlumberger arrays with profile lengths between 112 and 280 meters. The interpretation of the electrical resistivity data using robust inversion methods indicated that the subsurface around a cave south of Springfield in southwest Missouri likely contains cave passages currently cut off from the main body of the cave by breakdown. The new cave passages are located to the west of the main cave just beyond breakdown associated with a sinkhole and directly to the northeast of the main cave. These new passages are located within approximately a meter of the known cave passages. These locations have been predicted and mapped for use by the caves owner to excavate to the new passages so that the new and old passages can be connected. Electrical resistivity geophysics allowed for an effective and noninvasive investigation into the area around the cave. This method could easily be used to the advantage of investigators in other sites in similar karst environments to discover and map the location of potential features like caves and sinkholes.

REFERENCES

- Ahmed, S., and Carpenter, P.J., 2003, Geophysical response of filled sinkholes, soil pipes, and associated bedrock fractures in thinly mantled karst, east-central Illinois: *Engineering Geology*, 44, 705-716
- Bates, Robert L., and Jackson, Julia A., 1984, *Dictionary of Geological Terms Third Edition: Library of Congress Catalog*, 280
- Beard, Jonathan B., 2019, Vadose Speleogenesis in the Pierson Limestone: *The Journal of the Missouri Speleological Survey*, 59
- Berglund, James L., Mickus, Kevin., Gouzie, Douglas., 2014, Determining a relationship between a newly forming sinkhole and a former dry stream using electric resistivity tomography and very low frequency electromagnetics in an urban karst setting: *Inspiration*, 2, SF17-SF27
- Berglund, James L., 2012, *An applied Karst Study of the Ward Branch Watershed Near the James River Freeway/South Campbell Interchange: Missouri State Graduate MS Thesis*
- Dahlin, Torleif., and Loke, M. H., 2018, Underwater ERT surveying in water with resistivity layering with example of application to site investigation for a rock tunnel in central Stockholm: *Near Surface Geophysics*, 16, 230-237
- Decker, Wayne L., 2022, *Climate of Missouri: University of Missouri, Missouri Climate Center*
- Evans, Kevin R., Jackson, Jeremiah S., Mickus, Kevin L., Miller, James F., Cruz, Dulce., 2011, *Enigmas and Anomalies of the Lower Mississippian Subsystem in Southwestern Missouri: Search and Discovery Article #50406*
- Ezma, Olisaemeka K., Ibuot, Johnson C., Obiora, Daniel N., 2020, Geophysical investigation of aquifer repositories in Ibagwa Aka, Enugu State, Nigeria, using electrical resistivity method: *Groundwater for Sustainable Development*, 11, 100458
- Florea, L., 2005, Using state-wide GIS data to identify the coincidence between sinkholes and geologic structure: *Journal of Cave and Karst Studies*, 67, 120-124
- Gao, Yongli., 2008, Spatial operations in a GIS-based karst feature database: *Environmental Geology* 54, 1017-1027
- Gouzie, D., and Pendergrass, G., 2009, Investigation and remediation of the 2006 Nixa, Missouri, collapse sinkhole: *Environmental and Engineering Geoscience*, 15, 13-27

- Kaufmann, G., Romanov, D., Nielbock, R., 2011, Cave detection using multiple geophysical methods: Unicorn Cave, Harz Mountains, Germany: *Geophysics*, 76, 71-77
- Land, L., 2011, Geophysical prospecting for new cave passages: Fort Stanton Cave, New Mexico, USA: National Cave and Karst Research Institute Report
- Loke, M.H., 1999, RES2DMOD version 2.2: rapid 2-D resistivity forward modeling using the finite-difference and finite-element methods: Report GeoTomo LLC
- Loke, M.H., 2020, *Electrical Resistivity Surveys and Data Interpretation: Encyclopedia of Solid Earth Geophysics*, Springer, Cham.
- Palmer, A., 1991, Origin and morphology of limestone caves: *Geological Society of America Bulletin*, 103, 1-21
- Peterson, T., and Berg, J., 2001, Karst mapping with geophysics at Mystery Cave State Park, Minnesota: DNR Waters Ground Water and Climatology Section
- Qiu, Xiaomin, Wu Shuo-Sheng, Chen, Yan., 2018, Sinkhole susceptibility assessment based on morphological, imagery, and contextual attributes derived from gis and imagery data: *Journal of Cave and Karst Studies*, 82, 1-17
- Roth, M., Mackey, J.R., Mackey, C., Nyquist, J.E., 2002, A case study of the reliability of multielectrode earth resistivity testing for geotechnical investigations in karst terrains: *Engineering Geology*, 65, 225-232
- Thompson, Thomas L., 1986, Paleozoic Succession in Missouri part 4 Mississippian System: Missouri department of Natural Resources Division of Geology and Land Survey, Report of investigation, 70
- Torrese, Patrizio., 2020, Investigating karst aquifers: Using pseudo 3-D electrical resistivity tomography to identify major karst features: *Journal of Hydrology*, 580
- White, W.B., 2002, Karst hydrology: recent developments and open questions: *Engineering Geology*, 65, 85-105
- Zhou, W., Beck, B.F., Stephenson, J.B., 2000, Reliability of dipole-dipole resistivity tomography for defining depth to bedrock in covered karst terranes: *Environmental Geology*, 39, 760-766
- Zhou, W., Beck, B.F., Adams, A.L., 2002, Effective electrode array in mapping karst hazards in electrical resistivity tomography: *Engineering Geology*, 42, 922- 928